UNIVERSIDADE DO VALE DO RIO DOS SINOS - UNISINOS
UNIDADE ACADÊMICA DE PESQUISA E PÓS-GRADUAÇÃO

PROGRAMA DE PÓS-GRADUAÇÃO EM GEOLOGIA

Nome do Autor: Celso Pagano Galli

Título: Evolution of an estuarine valley to barrier-lagoon system promoted by tidal prism change during a transgressive event (Lower Permian, Paraná Basin)

Nível: Mestrado

Data de Defesa: 27/11/2020

E-mail de Contato do Autor: celsopgalli@gmail.com

UNIVERSIDADE DO VALE DO RIO DOS SINOS - UNISINOS
UNIDADE ACADEMICA DE PESQUISA E PÓS GRADUAÇÃO
PROGRAMA DE PÓS GRADUAÇÃO EM GEOLOGIA
NÍVEL MESTRADO

DISSERTAÇÃO DE MESTRADO

EVOLUTION OF AN ESTUARINE VALLEY TO BARRIER-LAGOON SYSTEM PROMOTED BY TIDAL PRISM CHANGE DURING A TRANSGRESSIVE EVENT (LOWER PERMIAN, PARANÁ BASIN)

CELSO PAGANO GALLI

São Leopoldo
2021

G168e Galli, Celso Pagano.
Evolution of an estuarine valley to barrier-lagoon system promoted by tidal prism change during a transgressive event (Lower Permian, Paraná Basin) / Celso Pagano Galli. – 2021.
17 f. : il. color. ; 30 cm.

Dissertação (mestrado) – Universidade do Vale do Rio dos Sinos, Programa de Pós-Graduação em Geologia, São Leopoldo, 2021.
"Orientador: Prof. Dr. Ernesto Luiz Correa Lavina."

1. Carvão. 2. Carvoeiros. 3. Geologia estratigráfica. 4. Paraná, Rio, Bacia. I. Título.

CDU 55

Dados Internacionais de Catalogação na Publicação (CIP)
(Bibliotecária: Bruna Sant'Anna – CRB 10/2360)

HIGHLIGHTS

- High-resolution sedimentological and stratigraphical analyses in core and outcrop.
- Decrease in the tidal prism throughout sedimentary infilling of an incised valley.
- Transition from tide-dominated estuary to wave-dominated coast.
- Candiota coal-bearing formation in a barrier-lagoon depositional system.

Journal of South American Earth Sciences 110 (2021) 103398

Contents lists available at ScienceDirect

Journal of South American Earth Sciences

journal homepage: www.elsevier.com/locate/jsames

Evolution of an estuarine valley to barrier-lagoon system promoted by tidal prism change during a transgressive event (Lower Permian, Paraná Basin)

Celso Pagano Galli, Joice Cagliari *, Ernesto Luiz Correa Lavina

Graduate Program in Geology, Unisinos University, Unisinos Av., 950, São Leopoldo, RS, 93322-750, Brazil

ARTICLE INFO

Keywords:
Tide
Wave
Coal-bearing
Incised valley
Rio Bonito Formation

ABSTRACT

In modern marine marginal environments, the coastal morphology directly influences the tidal and wave processes. In this paper we present an example of an ancient coastal zone where the change in coastal morphology controlled the tidal range. This study focuses on the Permian Rio Bonito Formation in the southern Paraná Basin, where the major coal deposits of South America are located. Sedimentological and stratigraphical approaches were applied to cores drilled in the Candiota paleovalley area. We describe the stratigraphic architecture of a transgressive event of the Lower Permian (Rio Bonito Formation). Two third order depositional sequences were identified, which show differences in the paleoenvironmental record. In the lower sequence, associated with the infilling of an incised valley, facies related to fluvial and tidal currents are dominant. In a micro-tidal inner sea context, tidal range is amplified in a funnel-shaped valley. In the upper sequence, already evolving in linear coastal conditions, evidence of tidal depositional processes almost disappear, and the sedimentation becomes dominated by wave processes, thus a coastal barrier system associated with lagoons and swamps is established. Our study, besides detailing the paleoenvironmental evolution of the sedimentary infilling of an incised valley, also provides for a better understanding of the origin of southern Brazil coal.

1. Introduction

Marginal-marine settings or coastal environments lie between the continental and the marine depositional domains, where river, tidal, and wave processes occur (Boyd et al., 1992, 2006, 2006; Boggs, 2006; Ainsworth et al., 2011). In transgressive settings, tidal range and wave height, as well as coast morphology and sediment supply source, control the development of tide- and wave-dominated coasts (Boyd et al., 2006; Dalrymple et al., 1992; Dalrymple and Padman, 2017). Transition from tide-to wave-dominated coast is explained by a reduction in the rate of the sea level rise in the Huelva coast, southwestern Spain, during the Holocene (Davis and Clifton, 1987; Pendón et al., 1998). This rate reduction caused the infilling of several local estuaries and consequently the decrease in the tidal prism, favoring the sand barrier formation.

Estuaries are complex environments and ephemeral depositional systems that commonly have a short time span. Modern estuaries for instance, are coastal features formed over the past 5000 to 6000 years during the stable interglacial period (Schubel and Hirschberg, 1978). Balance between fluvial and marine sediment input and the relative sea-level rise control the estuary evolution. If fluvial or marine sediment input occur at higher rates than sea-level rise, delta and prograding coasts are formed (beach ridges or strand plains if wave energy is dominant, and open coast tidal flats if tidal energy is dominant), on the contrary, if sea-level rises at higher rates, then a new estuary might be formed (Dalrymple et al., 1992, 2012, 2012; Dalrymple and Choi, 2007; Ainsworth et al., 2011).

The deglaciation phase of the Late Paleozoic Ice Age – LPIA caused the sea level rise and a transgressive event recorded in several basins of the southern Gondwana (Milani et al., 2007; Mottin et al., 2018). The Rio Bonito Formation of the Paraná Basin, deposited in the Early Permian (Cagliari et al., 2016; Griffis et al., 2018; Rocha-Campos et al., 2019), is interpreted as being deposited in coastal environments during this transgressive phase (Lavina and Lopes, 1987; Lopes, 1995; Holz, 2003; Gandini et al., 2010; Schmidt-Neto et al., 2018; Trentin et al., 2019; Maahs et al., 2019). In the southern basin, this unit is thicker within some paleovalleys (e.g., Capané and Candiota; Aboarrage and Lopes, 1986; Lopes, 1995, 2004). Sedimentary facies of the Rio Bonito Formation are interpreted as deltaic, estuarine, and barrier-lagoon systems, developed in a shallow marine environment (Lavina et al., 1985; Lavina and Lopes, 1987). However, recent studies performed by Fritzen

* Corresponding author.
E-mail address: joiceca@unisinos.br (J. Cagliari).

https://doi.org/10.1016/j.jsames.2021.103398
Received 25 November 2020; Received in revised form 30 April 2021; Accepted 22 May 2021
Available online 29 May 2021

et al. (2019) and Candido et al. (2020) characterize the tidal control on sediment deposition in proximal areas of Capané and Candiota paleovalleys and indicate a meso- to macro-tidal range depositional environment possibility.

The purpose of this study is to document the tidal influence on sediment deposition and its control over depositional systems throughout the lower Permian succession of the southern Paraná Basin (Candiota paleovalley area). The focus is on the study of well cores and outcrops of the Rio Bonito Formation, in southern Brazil. A high-resolution approach allowed us to obtain new insights of the depositional environment evolution. The results point to a significant change in the depositional processes, from a highly cutoff coastal morphology controlled by tide in the lower section, to the establishment of a wave-dominated linear coast in the upper section.

2. Geological setting

The Paraná Basin is a great (~1,500,000 km^2) intracratonic sedimentary basin located in the South American continent. Its deposits can mainly be found in Brazil, but they can also be observed in Paraguay, Uruguay and Argentina (Zalán et al., 1990; Milani et al. 1998, 2007). Its sedimentary history is comprised of 6 s-order depositional sequences (supersequences) that are limited by interregional discordances: Rio Ivaí (Ordovician to Silurian), Paraná (Devonian), Gondwana I (Carboniferous to Early Triassic), Gondwana II (Early to Middle Triassic), Gondwana III (Early Jurassic to Early Cretaceous), and Bauru (Early Cretaceous) (Milani et al., 2007). The first three supersequences are transgressive-regressive cycles controlled by relative sea level changes, while the other three correspond to continental sedimentary rock packages associated with igneous rocks (Zalán et al., 1990; Milani et al., 2007).

During the Late Devonian and Mississippian, tectonic factors and/or a relative sea level fall due to glaciation generated a large gap in the Paraná Basin sedimentary record (Milani et al., 2007). Following this hiatus, sedimentation resumed during the Pennsylvanian after the northward progressive Gondwana migration and at the beginning of the deglaciation process (Lavina and Lopes, 1987; Milani et al., 2007). This sedimentary record is preserved in the Itararé Group and the Aquidauana Formation. During the Early Permian, post-glacial deposition was recorded in the Guatá Group (Rio Bonito and Palermo formations) (Lavina et al., 1985; Lopes and Lavina, 2001).

The Rio Bonito Formation, at the base of the Guatá Group, was deposited in an estuarine and barrier-lagoon paleoenvironment, under fluvial and tidal influence in the basal succession, and wave influence in the uppermost succession (Lavina and Lopes, 1987; Holz, 2003). It has been extensively studied in southern Brazil due to its coal reserves, the genesis of which is associated with different depositional environments, such as deltas, estuaries, coastal-barriers and marsh-lagoon systems (Lavina et al., 1985; Lopes and Lavina, 2001; Lopes et al., 2003a, b; Jasper et al., 2006; Buatois et al., 2007; Gandini et al., 2010, Candido et al., 2019; Trentin et al., 2019).

The Rio Bonito Formation radiometric dating reveals ages from Asselian to the Artinskian (see summary in Cagliari et al., 2014, and recent results published by Cagliari et al., 2016; Griffis et al., 2018; and Rocha-Campos et al., 2019). For the Candiota area, high-resolution single zircon CA-TIMS results of previously dated tonstein deposits are older and suggest a shorter time span for the Rio Bonito Formation. According to Griffis et al. (2018) the oldest age is 298.23 ± 0.31 Ma (Asselian) for the lower Candiota coal seams, and the youngest age is 297.77 +0.35/-0.59 Ma (Asselian) for the Hulha Negra tonstein, stratigraphically positioned above the upper Candiota coal seams.

In the study area, the Candiota paleovalley (Holz, 1999, 2003, 2003; Holz et al., 2006) records a funnel-shaped estuary that opened to the sea in the south, being approximately 50 km wide in its southern region and 15 km wide in its northern, more proximal area (Holz, 2003). Overlying the Itararé Group the Rio Bonito Formation in the paleovalley records four main depositional systems: alluvial fan, fluvial-dominated delta, lagoonal estuary, and barrier island (Holz, 2003). In the Trentin et al. (2019) study, this succession comprises fluvial-estuarine deposits followed by a barrier-lagoon system. Offshore deposits of the Palermo Formation occur on top of the barrier-lagoon system deposits. A recent study developed by Fritzen et al. (2019) in the Candiota paleovalley recognized a semi-diurnal tidal regime in the tidal-influenced deposits near the estuary head. Mathematical scenarios performed by Candido et al. (2020) revealed that tidal amplification was likely in this valley, producing micro- to mesotidal conditions and controlling sediment deposition.

3. Material and methods

The studied area covers approximately 7000 km^2 in the state of Rio Grande do Sul, in southern Brazil (Fig. 1). It is located in the Candiota paleovalley, on the southeastern border of the Paraná Basin. This study is based on 33 of ~750 wells in this portion of the basin, drilled by the Brazilian Geological Survey (CPRM) (Tab. SM1 of supplementary material). The 33 cores were used to perform four stratigraphic sections, from which 22 were described in high-resolution for facies analysis, and for the remaining wells, the original logs were used as reference. For the facies analysis, physical (lithology, sedimentary structures and boundaries) and biogenic attributes (presence and/or evidence of organisms or fragments) were described. Facies geometry and paleocurrents, as well as other detailed attributes were obtained from nine outcrops (Tab. SM2 of supplementary material and Fig. 1).

Stratigraphic sections were elaborated following the conceptual premises of sequence stratigraphy *sensu* Catuneanu et al. (2009, 2011). For the stratigraphic correlation, we have analyzed the vertical succession of facies and the gamma ray logs in four sections. Section 1 is a dip section (84 km long, N–S direction) and the other three are strike sections with a NW-SE direction (43.1 km, 19.6 km, and 27.7 km long for sections 2, 3 and 4, respectively) (Fig. 1). Complete stratigraphic sections with a detailed sedimentary log are available in the supplementary material (Fig. SM1 to SM4). The datum used for logs correlation is located on carbonaceous facies, which corresponds to a marker in most gamma ray logs. Due to the absence of a prominent marker, the datum was reached by adjusting the carbonaceous segment at the bottom of sequence 2 in different wells of the strike north and dip sections (Figs. 12 and 9). In the northern section, the datum is positioned on a radioactive peak over which there is a reduction followed by an increase in the gamma with the shape of a handsaw tooth. This feature is prominent in the eastern and central sectors of the northern section, losing expression in an easterly direction. However, the observation of the general behavior of the gamma ray curve below and above this radioactive peak, as well as the horizontalization of the base of the upper sandy sequence (gamma rays with box pattern), makes it possible to track it with confidence. In the dip section the same pattern can be defined in the north and central sectors.

The paleobasement morphology of the Candiota Paleovalley was modeled based on 53 logs, taking into consideration the same datum used in the stratigraphic sections (Tab. SM3). This model reflects the basement morphology in the upper part of Depositional Sequence 1 of the Rio Bonito Formation.

4. Results

4.1. Paleobasement model

The paleobasement model in upper Depositional Sequence 1 of the Rio Bonito Formation (see item 4.3) reveals the existence of a funnel shaped valley more than 90 km in length. The paleovalley mouth, in the south, is about 50 km wide and 96 m deep in the deepest portion (AG-01). The paleovalley head, in the north, is 20 km wide and has a depth of 35 m (Fig. 2). The valley morphology is irregular, both in the base and

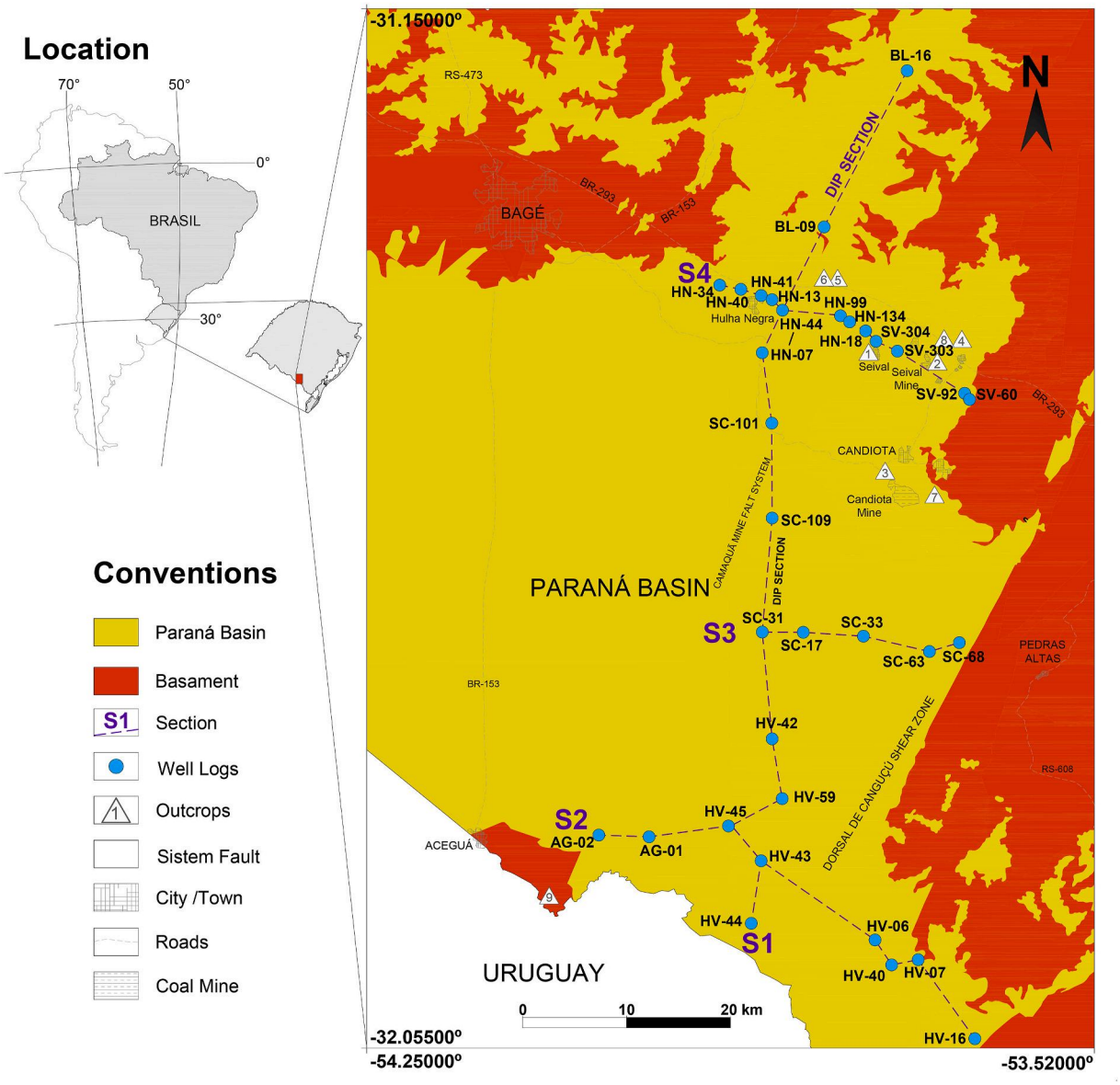

Fig. 1. Simplified geological map of the study area in southern Brazil (Wildner et al., 2006) with well, outcrops, and stratigraphic sections (S1 to S4) location.

margins, caused by tectonic compartmentation.

In the paleobasement model, the depression identified in the southern portion (AG-02, AG-01, HV-45 and HV-43) advances sinuously to the central portion (Fig. 2). There is a significant straight in the north valley, located at 31.4°S (HN-18, HN-134 and HN-304).

4.2. Facies and facies association

Eighteen sedimentary facies were described in the study area and grouped into five facies associations: I) Fluvial; II) Central Estuary; III) Lower Estuary; IV) Back-barrier, and V) Barrier (Table 1).

4.2.1. Fluvial facies association

4.2.1.1. Description. This facies association includes two sedimentary facies: trough cross-bedding conglomerate (Gtf) and trough cross-bedding arkosic sandstone (Stf) (Fig. 3). The Gtf facies has a conglomerate sedimentary composition, from granule to pebble, with polymictic clasts, while the Stf facies is composed of fine-to very coarse-grained arkosic sandstone. The Gtf and Stf facies occur, in this order, at the base of the valley in southern or nearby the southeast valley wall, mainly overlying Dm facies, but occur locally over the crystalline basement and intercalated with the central estuary, barrier, and back-barrier facies association. At the base of the valley, thickness reaches up to 6 m, but when intercalated with other facies associations, the thickness ranges between 0.5 and 4 m.

4.2.1.2. Interpretation. The Gtf and Stf facies represent 3D dunes under a unidirectional lower flow regime. The polymictic and feldspar composition of this facies indicates limited transport and reworking, characterizing a fluvial source of sediment and a proximal position. The superimposition of 3D dunes is associated with transversal or lingoid bars (Stf facies) and gravel bars (Gtf facies) that infill fluvial channels (Miall, 1977, 2006; Collinson, 1970, 1996; Pyrcz, 2015; Boggs, 2006; Yeste et al., 2018). The related debris flow deposits (Dm facies), suggest the existence of steep slopes and periods of intense rainfall (Iverson, 1997, 2009; Takahashi, 2007, 2009; Eyles and Kocsis, 1988).

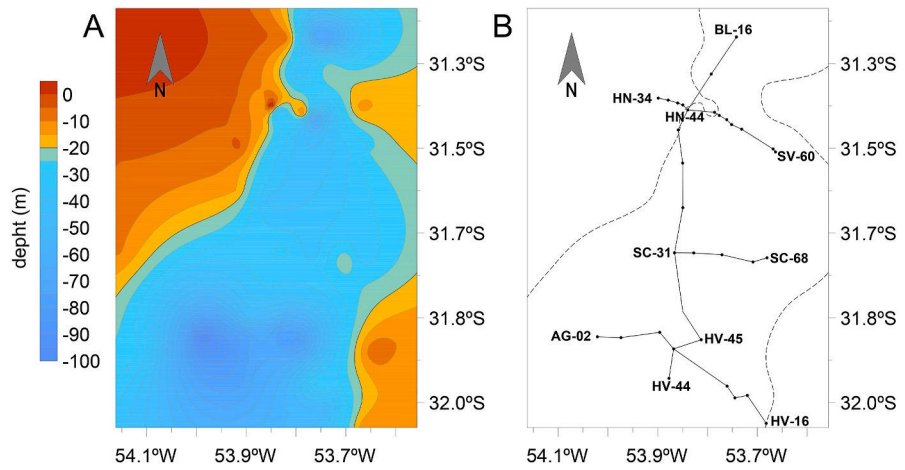

Fig. 2. A) Basement morphology model at the time of upper Depositional Sequence 1 and the Candiota Paleovalley configuration. Contour lines reflect thickness measured from the datum with contour interval of 10 m. B) Location of the stratigraphic sections in the paleovalley (S1 to S4).

4.2.2. *Central estuary facies association*

4.2.2.1. Description. This facies association includes four sedimentary facies: trough cross-bedding arkosic sandstone (Stf), trough cross-bedding arkosic sandstone with mud drapes (Stfmd), trough cross-bedding arkosic sandstone with wave ripples (Stfw), and heterolith (Ht) (Fig. 4). Stfmd and Ht facies are predominant, while Stfw and Stf are subordinate in this facies association. The matrix-supported conglomerate facies (Dm) is locally interbedded. This facies association is overlying the crystalline basement, Itararé Group rocks, or fluvial facies association. The vertical succession of facies is usually erosive-based and finning-upward, formed from base to top, by Stf, Stfmd, and Ht. Sandy facies (Stf, Stfmd, and Stfw) occur as lenticular packages within heterolith facies (Ht). This facies association is mostly preserved in the north of the study area, reaching up to about 60 m in Section 4, but it is also significantly thick in the central area and shows a small occurrence in the south, with thickness ranging between 13 and 18 m. In the central area, this facies association is intercalated with the lower estuary facies association (see Section 1).

Sedimentary facies were grouped since they share similar sediment composition, texture, and primary sedimentary structures. Sandier facies have an arkosic composition and are poorly sorted, with angular to sub-rounded grains. The predominant sedimentary structure in sandstone is the trough cross-bedding or cross-lamination, with mud drapes, and sigmoidal reactivation surfaces. Furthermore, the Stfmd facies presents herring-bone cross stratification and preferential paleocurrent SW-W and SW-S in outcrops 3 and 7 (see Fig. 1 and 4).

4.2.2.2. Interpretation. Sediment composition and texture indicate limited transport and reworking, similar to the fluvial facies association, therefore, compatible with fluvial input. The main primary sedimentary structures of these facies record the transport of sediment under a lower flow regime, and the occurrence of mud drapes, as well as sigmoidal reactivation surfaces and herring-bone cross-stratification are evidence of tidal action (Collinson et al., 2006; Dalrymple and Choi, 2007; Longhitano et al., 2012). Paleocurrents show seaward sediment transport, representing the fluvial joining with the ebb-tidal current, and reactivation surface, as well as herring-bone cross-stratification and the reverse flow (flood current) (Dalrymple and Choi, 2007). The predominance of Stfmd facies reflects an environment in which fluvial energy is important, but with the occurrence of slack-water periods and reverse flow. Subordinate occurrence of Stf facies reinforces the occurrence of fluvial processes in the same sub environment (Leuven et al., 2018).

The occurrence of erosive-based and finning-upward sand packages with lenticular geometry within heterolith facies point out to broad mud plains eroded by meandering channels (Boggs, 2006; Dalrymple et al., 2012; Leuven et al., 2018). The constant presence of tidal evidence in the channel fill deposits is the key feature which identifies this facies association as the record of sediment deposition taking place in the central estuary (or fluvial-tidal transition zone), in which sediment is supplied by rivers where both fluvial and tidal processes occur (Dalrymple et al., 1992, 2012; Dalrymple and Choi, 2007). In this zone, the ebb tide is the dominant current and flood tide the subordinate current (Fritzen et al., 2019). The Dm facies, interbedded in this facies association represents debris flow deposits, suggesting the presence of steep slopes and periods of intense rainfall (Iverson, 1997, 2009; Takahashi, 2007, 2009; Eyles and Kocsis, 1988).

4.2.3. *Lower estuary facies association*

4.2.3.1. Description. This facies association includes four sedimentary facies: trough cross-bedding quartz-rich sandstone with mud-drapes (Sttmd), horizontal lamination quartz-rich sandstone (Sht), heterolith (Ht), and bioturbated heterolith (Hw) (Fig. 5). It is distributed in the central and south area, reaching up to 26 m of thickness in Section 3, however, is absent in the north where the central estuary facies association occurs. In the E-W direction (Section 2), it has more than 43 km of lateral continuity. It is overlying crystalline basement, Itararé Group rocks or fluvial facies association in the south, and central estuary facies association in the central area.

The Sttmd and Sht facies are composed of very fine-to fine-grained quartz-rich sandstone with well sorted, sub-rounded to rounded grains. The sedimentary structure is trough cross-bedding with mud drapes for Sttmd and horizontal lamination for Sht facies. Sttmd facies predominates in the central portion (Section 3), in which Ht facies is distributed laterally, next to the valley border. In the south area (Section 1 and 2), bioturbated heterolith facies (Hw) occur interbedded with the Sttmd and Sht facies. This facies association was described only in cores; therefore, paleocurrent measurements are not available.

4.2.3.2. Interpretation. Sedimentary composition and texture of sandstone facies are indicative of long transport and reworking, suggesting sediments are supplied by longshore current (littoral drift input, McCubbin, 1982; Leuven et al., 2016, 2018). Depositional sedimentary structures record turbulent, strong current flows, and slack-water periods. All these characteristics, added to the distribution of this facies association in the south and central areas, suggest a lower estuary zone (or outer estuary), where marine sediment is transported landward by

Table 1
Description and interpretation of the Rio Bonito Formation sedimentary facies.

Code	Name	Description	Sedimentary processes	Environment/ Facies Association
Dm	Diamictite	Matrix-supported conglomerate; massive; muddy-sandy matrix; gravel to pebble polymictic clasts (quartz, granite, gneiss, and andesite); angular and rounded clasts; packages range from 0.3 to 6 m in thickness.	Debris Flow. Gravity flow on steep slopes (Takahashi, 2007, 2009, 2009; Iverson, 1997, 2009, 2009; Eyles and Kocsis, 1988).	
Gtf	Trough cross-bedding conglomerate	Granule to pebble conglomerate; clast-supported; cross-bedding; normal grading and clasts imbrication. Clasts are polymictic (quartz, granite, gneiss, and andesite) and angular to sub-rounded. Packages range between 0.5 and 4 m in thickness.	Dune under unidirectional lower flow regime composing gravel bars of fluvial channel fill (Miall, 1977; Collinson, 1970; Collinson et al., 2006; Pyrcz, 2015; Yeste et al., 2018).	Fluvial Fluvial and Central estuary
Stf	Trough cross-bedding arkosic sandstone	Fine- to very coarse-grained arkosic sandstone; angular to sub-rounded grains; poorly sorted; cross-bedding (sets of 10–35 cm in height). Packages range between 0.5 and 4.8 m in thickness.	Superimposition of dune under unidirectional lower flow regime composing transverse or linguoid bars (Miall, 1977; Collinson, 1970; Collinson et al., 2006; Yeste et al., 2018; Best and Fielding, 2019).	
Stfmd	Trough cross-bedding arkosic sandstone with mud drapes	Fine- to very coarse-grained arkosic sandstone with gravel; angular to sub-rounded grains; poorly sorted; trough cross-bedding (sets of decimetric heights) with carbonaceous mud-drape in the foresets; SW-W and SW-S paleocurrent. Associated rocks with large-scale sigmoidal erosive surfaces; ripple cross-lamination; plant debris, root horizon, and thin paleosoil. Rare herring-bone cross-stratification also occurs. Tabular to lenticular geometry with flat scoured base (outcrops 3 and 7). Core, packages of this facies exceed 15 m in thickness.	3D dunes under unidirectional lower flow regime with mud drapes indicating slack-water periods (Miall, 1977; Collinson et al., 2006). Grain composition and texture indicate fluvial source of the sediment. Reactivation surfaces indicate the occurrence of reversal flow, and rare herring-bone stratification and the presence of bimodal currents (Dalrymple and Choi, 2007; Longhitano et al., 2012). Channeled tidal bar (Dalrymple et al., 1992, 2012, 2012; Longhitano et al., 2012; Fritzen et al., 2019).	Central estuary
Stfw	Trough cross-bedding arkosic sandstone with wave ripples	Fine-grained arkosic sandstone; sub-rounded grains; well sorted; trough cross-bedding (sets of decimetric height); symmetrical ripples in the cross-bedding foresets; SE paleocurrent is dominant and NW paleocurrent is subordinate; large-scale sigmoidal erosive surfaces occur. A 2.5 m thick package showing lenticular geometry with concave-up base. Facies only described in outcrop 8.	3D dunes under unidirectional lower flow regime with bimodal paleocurrents (Miall, 1977; Collinson, 1996; Collinson et al., 2006). Reactivation surface indicates the occurrence of reversal flow (Dalrymple and Choi, 2007; Longhitano et al., 2012). Symmetrical (or wave) ripples in the cross-bedding foresets indicate oscillatory flow during slack-water periods (Collinson et al., 2006). Tidal bar with influence of oscillatory flow (Dalrymple et al., 1992, 2012, 2012; Tape et al., 2003; Dalrymple and Choi, 2007; Longhitano et al., 2012).	
Ht	Heterolith	Fine- to very fine-grained sandstone (80–95%) and siltstone; ripple cross-lamination in the sandstone with wavy and flaser bedding; plant debris are common; bioturbation is weak to moderate (bioturbation index 1–3) or locally absent. Packages reach up to 10 m thick (see AG-01, HN-44, HN-18, SV-304, BL-19).	Mud decantation during quiescence periods and sand transport episodes by weak currents (Collinson et al., 2006; Flemming, 2012). Mixed flat: accretion at top and lower portion of tidal bars (Clifton, 1976; Wiberg and Harris, 1994; De Boer et al., 1989; Bann et al., 2014; Mángano and Buatois, 2014; Daidu, 2013).	Central and Lower estuary
Sht	Horizontal lamination quartz-rich sandstone	Very fine-grained quartz-rich sandstone with rounded and well sorted grains, with horizontal lamination, the sedimentary structure is absent locally, and bioturbation is moderate to intense marked by thin obliterated mud laminae. Occurrence associated with small-scale cross-bedding with rare mud drapes (Sttmd).	Plane bed under upper flow regime (Collinson et al., 2006). Mud laminae obliterated by bioturbation could represent mud drape formed during slack water (Collinson et al., 2006; Flemming, 2012). Moderate to intense bioturbation indicates favorable conditions for infauna (MacEachern et al., 2010). Subtidal sand flat (Desjardins et al., 2012; Dalrymple and Choi, 2007).	Lower estuary
Sttmd	Trough cross-bedding quartz-rich sandstone with mud-drapes	Fine-grained quartz sandstone with rounded and well sorted grains; trough cross-bedding (sets of 10–25 cm in height); mud-drapes in the foresets of cross-bedding. No paleocurrent measurements. Facies described only in cores. Packages reach up to 20 m in thickness.	Superimposition of 3D dunes under unidirectional lower flow regime with mud drapes indicating slack-water periods (Miall, 1977; Collinson et al., 2006). Sediment composition and texture indicate marine source. Tidal bar (Dalrymple et al., 1992, 2012, 2012; Dalrymple and Choi, 2007; Longhitano et al., 2012).	
F	Mudstones	Light- to dark-grey claystone and siltstone; massive; tabular geometry; plant debris, root horizons, and thin paleosoils layers are common. Associated with lenticular beds of Stf facies. Locally, centimetric (<7 cm) horizons of volcanic ash (tonstein). Decimetric thickness sucession.	Fine-grained sediment decantation (Collinson et al., 2006; Flemming, 2012). Paleosoil and root horizons indicate episodic subaerial exposure (Daidu, 2013). Mud flats (Le Hir et al., 2011; Flemming, 2012; Daidu, 2013).	Back-barrier
Fc	Carbonaceous mudstone	Dark-grey claystone and siltstone; horizontal lamination; tabular geometry; plant debris. Locally, centimetric (<7 cm) horizons of volcanic ash (tonstein). Decimetric thickness (see SV-304).	Fine-grained sediment decantation Collinson et al., 2006; Flemming, 2012). Organic matter is preserved in anoxic conditions. Lagoon and swamp (Schnurrenberger et al., 2003; Le Hir et al., 2011; Flemming, 2012).	
C	Coal	Decimetric and metric coal beds with plant impression and pyrite nodules, and tabular geometry (outcrops 2, 4, and 5).	Organic matter accumulation in an oxygen poor freshwater environment, with abundance of vegetation, and rare influence of seawater (swamp, Schopf, 1956; Casshyap, 1970; Clemmensen and Surlyk, 1976; Silva and Kalkreuth, 2005).	

(*continued on next page*)

Table 1 (*continued*)

Code	Name	Description	Sedimentary processes	Environment/ Facies Association
Shwf	Horizontal lamination quartz-rich sandstone	Fine-grained quartz-sandstone; rounded grains; well sorted, horizontal lamination; locally, coarse-grained sandstone laminae; locally, root horizons and plant debris; lithified and pyritized layers; packages 0.7–3.5 m in thickness; associated with facies F and C. In outcrop 3, geometry is lenticular.	Plane bed under upper flow regime (Collinson et al., 2006). Washower fan (McCubbin, 1982; Shaw et al., 2015).	Barrier
Shw	Swash cross-stratification quartz-rich sandstone	Fine-grained quartz sandstone; rounded grains; well sorted; horizontal lamination and parallel lamination with low-angle dip (swash cross-stratification); packages are thicker than 10 m (see AG-02, AG-01, and HV-45 in Fig. 10).	Plane bed under upper flow regime (Collinson et al., 2006). Foreshore/swash zone (Harms et al., 1982; McCubbin, 1982; Van de Meene et al., 1996; Johnson and Baldwin, 1996; Masselink and Puleo, 2006; Anthony and Aagaard, 2020).	
Stw	Trough cross-bedding quartz-rich sandstone	Fine- to coarse-grained quartz sandstone; rounded grains; well sorted; trough cross-bedding (sets of 10–20 cm in height); wave-ripple cross-laminations are present next to the erosional surfaces. Outcrop 9 shows dominant NE paleocurrent and subordinate NW paleocurrent. Succession reaches up to 5 m in thickness, exceptionally 20 m (see HV-43 in Fig. 10).	3D dune under unidirectional turbulent flow (Miall, 1977; Collinson, 1996; Collinson et al., 2006). The erosive surfaces with wave-ripples indicate episodic wave interaction (Van de Meene et al., 1996). Upper shoreface (surf zone) influenced by longshore current (McCubbin, 1982; Elliot, 1986; Myrow and Southard, 1991; Collinson et al., 2006; Pemberton et al., 2012; Anthony and Aagaard, 2020).	
Sha	Inverse grading horizontal lamination sandstone	Fine- to medium-grained quartz sandstone; well sorted; high sphericity and opaque grains; subcritical climbing translatent with inverse grading; package reaches up to 0.5 m thick; associated with facies F and C.	Plane bed under upper flow regime (Collinson et al., 2006). Sand transport in saltation and grain collisions (translatent wind-ripple deposits) with inverse grading indicates grain flow processes (Kocurek, 1991). Eolian sand sheet (Kocurek and Dott, 1981; Kocurek and Nielson, 1986; Lancaster, 1995).	
Shcs	Hummocky cross-stratification sandstone	Very fine- to fine-grained sandstone; rounded grains; well sorted; hummocky Cross-stratification and wave-ripple cross-lamination (asymmetrical and symmetrical); rare interlayers of dark-grey siltstone laminae; weak bioturbation (bioturbation index 0–1). Succession thickness is greater than 30 m and displays tabular geometry (outcrops 1 and 6).	Complex bedforms generated during oscillatory flow or combined flow (Heward, 1981). Hummocks are formed above the storm-weather wave base and wave ripples above the fair-weather wave base. Lower shoreface to offshore transition (Harms et al., 1982; Cheel and Leckie, 1993; Dumas and Arnott, 2006; Anthony and Aagaard, 2020).	Barrier/Lower Shoreface
Sm	Massive sandstone	Medium- to coarse-grained sandstone with gravel; massive; beds with thicknesses between 1 and 25 cm; interbedded with Shcs facies.	Suspension transport during storm events. Lower shoreface to offshore transition (Clifton, 1976; Raaf et al., 1977; Wiberg and Harris, 1994; Greenwood, 2006; Leckie and Walker, 1982).	
Hw	Bioturbated heterolith	Very fine- to fine-grained sandstone (80%) and dark-grey, grey and greenish siltstone (20%); wavy and linsen bedding; 4–6 bioturbation index; succession reaches up to 20 m in thickness with tabular geometry (outcrops 1 and 6).	Decantation and sediment transport by waves. Transition zone between lower shoreface and offshore (Clifton, 1976; Raaf et al., 1977; Wiberg and Harris, 1994; Greenwood, 2006; Bann et al., 2014).	

tidal currents (Dalrymple et al., 1992, 2012; Boyd et al., 1992; Dalrymple and Choi, 2007). In this zone, the tidal maximum produces strong tidal currents and upper flow sand flats (Dalrymple et al., 1992; Dalrymple and Choi, 2007), deposited in the lower intertidal or subtidal areas (Desjardins et al., 2012). The occurrence of moderate to intense bioturbated heterolith indicates better environmental conditions, and likely higher salinity levels (MacEachern et al., 2010).

4.2.4. *Back-barrier facies association*

4.2.4.1. Description. This facies association includes six sedimentary facies: mudstone (F), carbonaceous mudstone (Fc), coal (C), trough cross-bedding arkosic sandstone (Stf), horizontal lamination quartz-rich sandstone (Shwf), and rare occurrence of heterolith (Ht) (Fig. 6). It is distributed in the north and central areas, reaching up to 38 m and 15 m in thickness (Section 4 and 3), respectively. In the south, it is restricted to a ~3 m thick succession. It is abruptly overlying central and lower estuary facies associations in the north and south portions, respectively, and is laterally related to the barrier facies association.

The F, Fc, and C facies are fine-grained rocks (siltstone, carbonaceous siltstone, claystone, and coal), massive or with horizontal lamination, and tabular geometry. In F and Fc facies, plant debris, root horizon, and paleosoil layers occur. A recurrent vertical succession is made up, from base to top by F facies which presents an increase in organic matter content (Fc) towards the top, and usually grades to a coal layer (C). Interbedded within these fine-grained facies, lenticular beds of Stf with a thickness of 0.3–4 m are present.

4.2.4.2. Interpretation. This facies association is composed of sedimentary facies recording fine-grained sediment and organic matter decantation in standing water conditions (Collinson et al., 2006; Flemming, 2012). Fine-grained facies (F and Fc) also record episodic subaerial exposure, typical of mudflats or lagoon margins (Reinson, 1992; Schnurrenberger et al., 2003; Le Hir et al., 2011). Organic matter accumulation (Fc and C) occurs in an oxygen-poor freshwater environment, with an abundance of vegetation, and rare influence of seawater (as marked by the presence of pyrite nodules; Smith and Batts, 1974; McCabe, 1985), interpreted as a swamp environment (Schopf, 1956; Casshyap, 1970; Clemmensen and Surlyk, 1976; Flores, 1978). Recurrent vertical succession records the establishment of a restricted lagoon with a progressive decrease in water depth, often with the development of swampy conditions at the top. Therefore, mudflats, lagoon, and swamp depositional environments are formed in a coastal plain. The lateral relation with barrier facies association indicates these depositional environments are placed in the back-barrier plain, separated from the sea by a coastal barrier (Reinson, 1992; Flemming, 2012). The back-barrier plain was probably under the seawater influence, as attested by the presence of pyrite nodules in coal facies. Intercalated with the fine-grained deposits of the back-barrier, are lenticular beds of horizontal lamination quartz-rich sandstone (Shwf) which are a

common occurrence, represent washover fan deposits associated with storm events (McCubbin, 1982; Nielsen and Nielsen, 2006; Shaw et al., 2015).

4.2.5. Barrier facies association

4.2.5.1. Description. This facies association is formed by seven sedimentary facies: horizontal lamination quartz-rich sandstone (Shwf), swash cross-stratification quartz-rich sandstone (Shw), trough cross-bedding quartz-rich sandstone (Stw), inverse grading horizontal lamination sandstone (Sha), hummocky cross-stratification sandstone (Shcs), massive sandstone (Sm), and bioturbated heterolith (Hw) (Figs. 7 and 8). The thickness of the vertical succession is greater in the south (reaching up to 46 m in Section 1 and 2) and less expressive in the north (less than 14 m in Section 4). Coarser grained sediments forming Stw, Shw, Shwf, and Sha facies mark the lower succession. In the upper succession, facies of Shcs, Sm, and Hw occur. This facies association is widely distributed and displays an abrupt and erosive basal contact with the underlying back-barrier and lower estuary facies association. Furthermore, its basal erosive surface is laterally associated with lower estuary facies association in the lowermost succession (Section 2) and with back-barrier facies association in the middle (Section 1).

Sandstone facies are very fine-to coarse-grained quartz sandstone with well-sorted and rounded grains. Horizontal lamination is a common sedimentary structure in Shwf, Shw, and Sha facies. In the Shw, horizontal and parallel lamination with a low angle dip show wedged-shaped sets with low-angle surfaces of truncation. Hummocky cross-stratification and wave-ripple cross-lamination are restricted to the very fine-to fine-grained sandstone facies (Shcs). In cores, hummocky cross-stratification is recognized by its low angle stratification with microgradation laminae.

4.2.5.2. Interpretation. The sediment composition and texture of sandstone facies indicate long transport and reworking, suggesting sediments are supplied by longshore current (littoral drift input). The lower succession, formed by Shw, Stw, and Shcs facies represents the foreshore, upper and lower shorefaces, respectively, recording a beach system (Clifton, 2006; Masselink and Puleo, 2006; Pemberton et al., 2012; Anthony and Aagaard, 2020). Hw and Shcs facies in the upper succession represent the transition zone between lower shoreface and offshore (Clifton, 1976; Raaf et al., 1977; Wiberg and Harris, 1994; Greenwood, 2006). The lateral succession of facies indicates the beach system coexisted with a lower estuary facies association, indicating a mixed energy domain (tidal and wave), followed by the establishment of a well-developed coastal barrier system (e.g. Elliott, 1986; Reinson, 1992; Johnson and Baldwin, 1996; Reading and Collinson, 1996; Li and Amos, 1999). The sandy barrier isolated back-barrier environments (mudflat, lagoon, and swamp) from the sea most of the time, however, during storm events it was partially destroyed, as recorded by washover fan deposits (Shwf facies, McCubbin, 1982; Shaw et al., 2015).

4.3. Sequence stratigraphy

The integrated analysis of the four stratigraphic sections allowed for the definition of two depositional sequences (1 and 2), which are boundary by subaerial unconformities (SB1 and SB2) (see Section 1-4, Figs. 9–12). Paleogeographic maps for specific intervals are shown in Fig. 13.

4.3.1. Depositional sequence 1

The thickness of Depositional Sequence 1 is variable because it is overlying different tectonic blocks, reaching up to 100 m in the paleo-depressions (see AG-01, Section 2, Fig. 10). It is mostly represented by tide-dominated central and lower estuary deposits and, secondarily, by fluvial and coastal barrier deposits. At the base of the valley there is a predominance of fluvial facies association. Tide-dominated lower estuary facies association (Section 1-3, Figs. 9–11) is mainly distributed between the central portion and the mouth of the valley, and the central estuary facies association (Section 1 and 4, Fig. 9 and 12) in the inner portion of the valley.

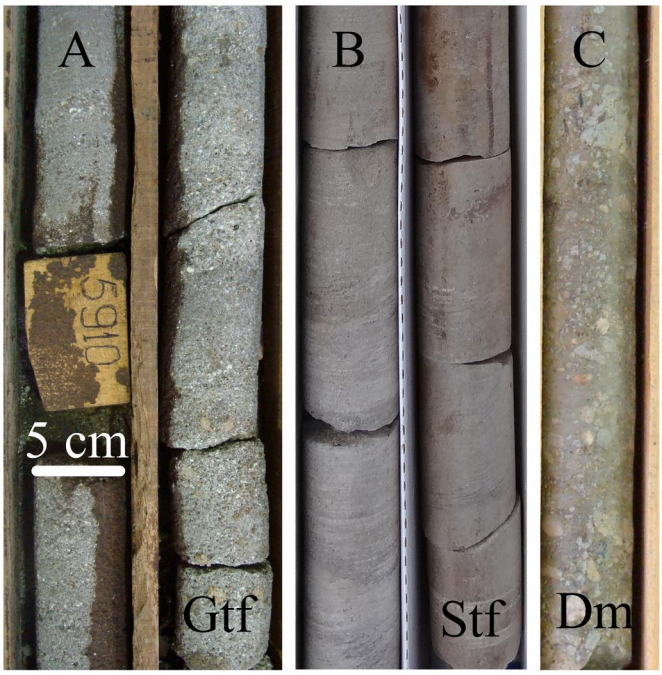

Fig. 3. Fluvial facies association and related diamictite. A) Trough cross-bedding conglomerate facies (Gtf) from SV-304, at 53 m depth. B) Trough cross-bedding arkosic sandstone facies (Stf) from AG-01, at 101 m depth. C) Diamictite facies (Dm) from SC-31, at 210 m depth.

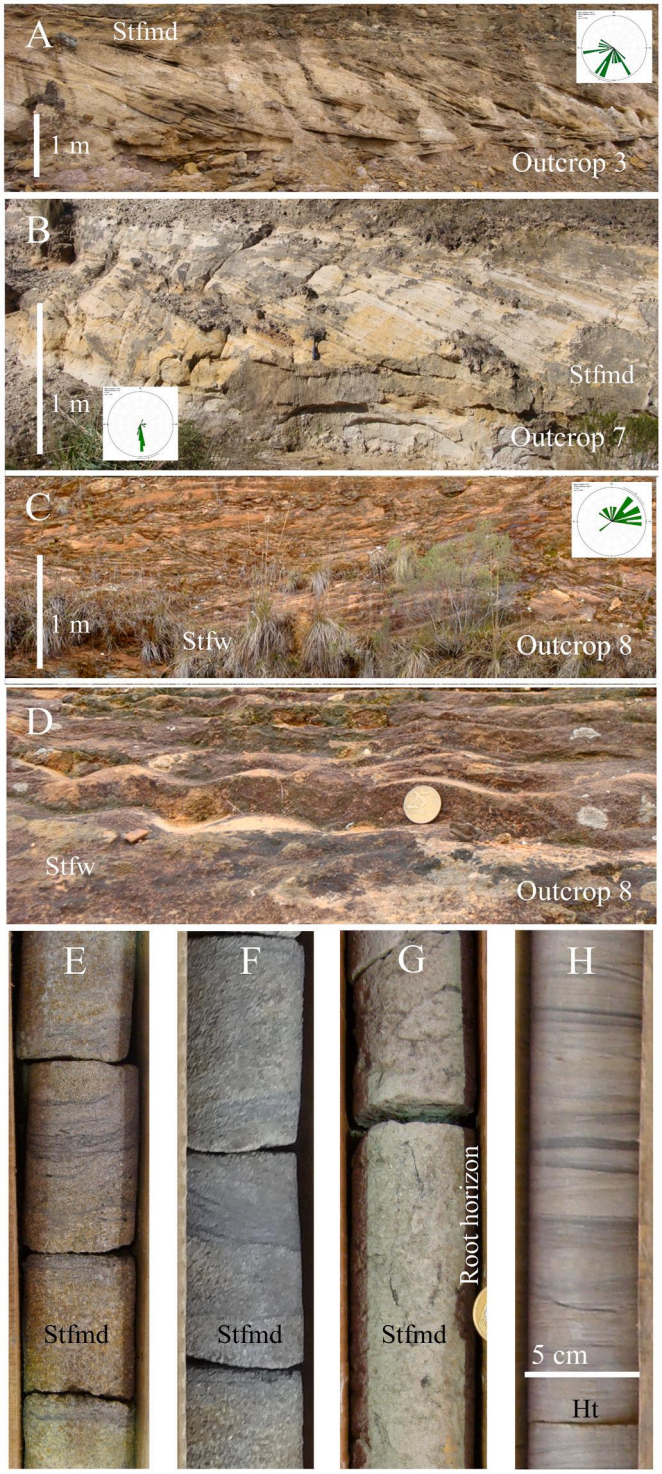

Fig. 4. Central estuary facies association. A-B) Trough cross-bedding arkosic sandstone of the facies Stfmd identified in the central-northeast area, near Candiota county (outcrops 3 and 7 location in Fig. 1). C) Trough cross-bedding arkosic sandstone of Stfw facies (outcrop 8). D) Detail of figure C showing wave ripples in the trough cross-bedding foresets. Coin with 2.2 cm in diameter to scale. E-F-G) Trough cross-bedding arkosic sandstone with mud drapes of Stfmd facies in core HN-44 (142.0 m in fig. E; 142.5 m in fig. F; 123.0 m in fig. G). Root horizon is shown in figure G, core HN-44 at 123 m depth. H) Heterolith facies (Ht) identified in core AG-01, at 90 m depth.

Fig. 5. Lower estuary facies association. A-B) Trough cross-bedding quartz rich sandstone with mud drapes facies (Sttmd), from core HV-43 (456.0 in the left core and 457.0 m in the right core at fig. A) and AG-01 (73 m, in fig. B). C) Heterolith facies (Ht) from core AG-01, at 91 m depth.

The basal sequence boundary (SB1) is a subaerial unconformity marked by the contact of Precambrian basement units (and the Pennsylvanian Itararé Group) with fluvial and estuarine deposits of the Rio Bonito Formation. The contact between Precambrian basement units and the Rio Bonito Formation represents a significant depositional hiatus (Milani et al., 2007; Holz et al., 2010; Tedesco et al., 2019). Fluvial deposits (Stf and Gtf) are preserved within the deepest incision of the valley and near the east valley wall (Section 2, Fig. 10). Overlying fluvial deposits, the estuarine succession presents sandy facies (Sttmd, Stfmd, Stfw) along the axis and hetherolithic facies (Ht) in both margins of the valley (Section 2, 3 and 4, Figs. 10–12). In the upper part of this sequence in the southern portion of the area, barrier facies (Stw, Shw, Shwf, Sha, Shcs, Sm and Hw) are well developed in the western area and migrate eastwards towards the top (Section 2, Fig. 10). The contact between fluvial and estuarine facies marks the tidal ravinement surface (TRS1), and the first appearance of the barrier overlying the estuarine facies marks the wave ravinement surface (WRS1) indicating landward shoreline migration (Section 1, Fig. 9). Syndepositional tectonic activity with the reactivation of old faults is recorded in lower Sequence 1 (Section 1, Fig. 9). Therefore, Depositional Sequence 1 records the low-stand system tract between SB1 and TRS1, restricted to the deepest portion of the valley, and the transgressive system tract between TRS1 and SB2.

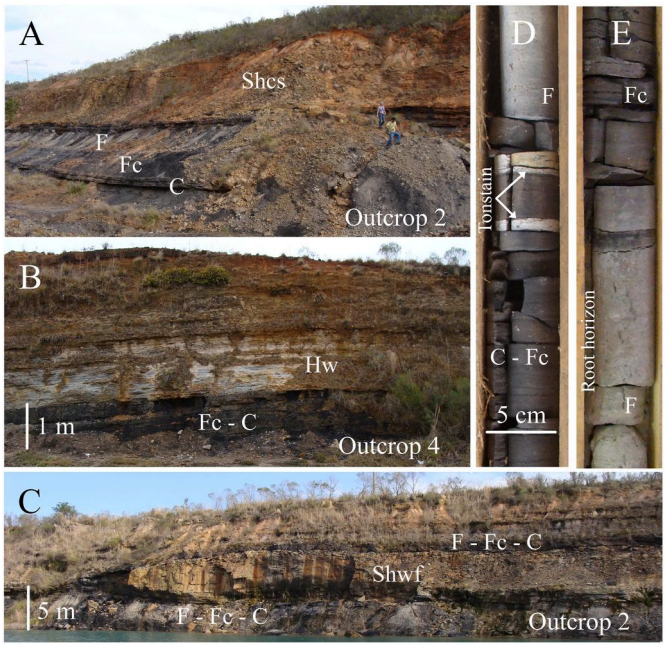

Fig. 6. Back-barrier facies association. A) Mudstone, carbonaceous mudstone and coal facies (F, Fc, and C) overlaid by wave ripple cross-lamination (Shcs facies), in outcrop 2. B) Carbonaceous mudstone and coal facies (Fc and C) overlaid by heterolith facies (Hw), in outcrop 4. C) Lenticular bed of horizontal lamination quartz-rich sandstone facies (Shwf) interbedded with F, Fc, and C facies in outcrop 2. D) Coal and carbonaceous mudstone facies (C and Fc) with whitish tonstein horizons (T) overlaid by mudstone facies (F), in core SV-303, at 15 m depth. E) Mudstone and carbonaceous mudstone facies (F and Fc) with root horizon in core SC-109, at 74 m depth.

4.3.2. Depositional sequence 2

The Depositional Sequence 2 thickness is about 50 m on average. It is mainly characterized by back-barrier, barrier, and offshore-transition deposits. Lenticular beds of fluvial deposits occur locally interbedded with the back-barrier and rarely in the barrier deposits.

The basal sequence boundary (SB2) is a subaerial unconformity and shows back-barrier and barrier deposits of Depositional Sequence 2 overlying estuarine deposits of Depositional Sequence 1. It is marked by fluvial incision and fluvial facies association in the southeast of Section 2 (Fig. 10) and by an irregular surface in Section 4 (Fig. 12). In the southern area, back-barrier facies (F, Fc, and C) are nearly absent (see Section 1-2, Figs. 9 and 10), whereas significant thickness (reaching up to 40 m in the BL-16-RS) occurs in the northeast (Fig. 9, 11 and 12), near the Candiota and Seival coal mines. In the central and north area, offshore-transition deposits are overlying back-barrier deposits and the barrier facies is nearly absent (Figs. 11 and 12). The dip section shows that there is a predominance of barrier and offshore-transition deposits in the south, and northward the back-barrier facies thickness increases and becomes dominant (Fig. 9). The contact between back-barrier (F, Fc and C) and barrier/offshore-transition (Shw, Stw, Shcs and Hw) facies marks the wave ravinement surface (WRS2), indicating the shoreline migration landward (Fig. 9). In the southwest, WRS2 is replacing SB2 (wells AG-02 and AG-01, Fig. 10). This depositional sequence records only the transgressive system tract.

5. Discussion

The analysis of the sedimentary succession preserved in the Candiota paleovalley reveals a significant change in the depositional environment throughout time, and hence a change in the dominant process controlling sediment deposition. In Depositional Sequence 1, on the distal part of the paleovalley, the sedimentation begins with fluvial deposits (Gtf

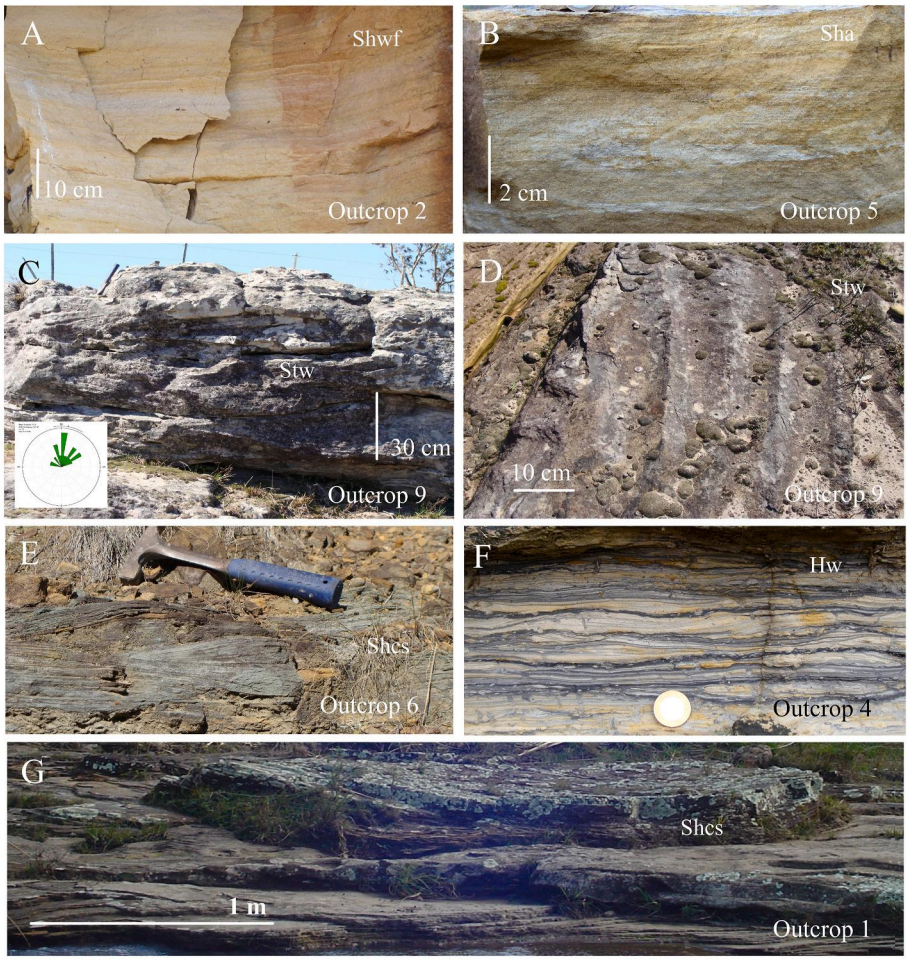

Fig. 7. Back-barrier and barrier facies associations. A) Horizontal lamination quartz-rich sandstone facies (Shwf) in outcrop 2. B) Inverse grading horizontal lamination quartz-rich sandstone facies (Sha) in outcrop 5. C) Trough cross-bedding quartz-rich sandstone facies (Stw) in outcrop 9. D) Detail of wave ripples associated with Stw facies, outcrop 9. E) Wave ripples cross-lamination (Shcs facies), in outcrop 6. F) Heterolith facies (Hw) with moderate bioturbation in outcrop 4. G) Hummocky cross-stratification sandstone facies (Shcs) in outcrop 1.

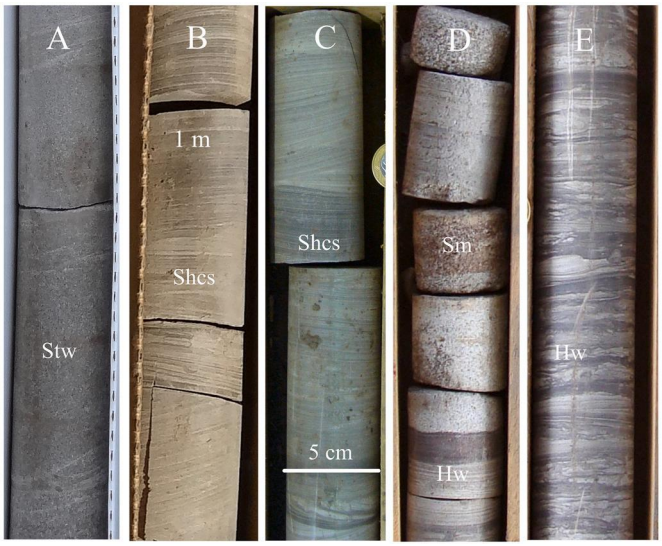

Fig. 8. Barrier facies association. A) Trough cross-bedding quartz rich sandstone faceis (Stw) in core HN-59, at 328 m depth. B–C) Hummocky cross-stratification sandstone facies (Shcs) in core HV-45 (at 171 m depth, in fig. B) and SC-109 (at 65 m depth, in Fig. C). D) Bioturbated heterolith facies (Hw) and massive sandstone faceis (Sm) in core HV-45, at 156 m depth. E) Bioturbated heterolith facies (Hw) in core HV-45, at 158 m depth.

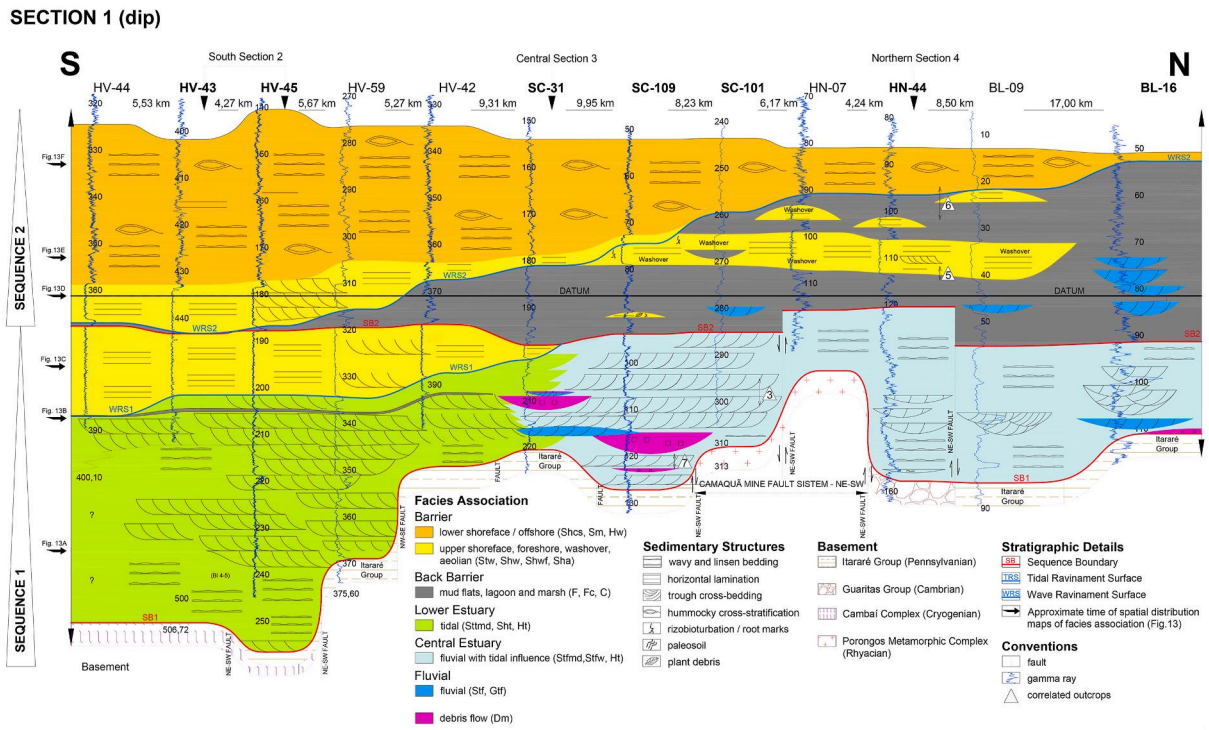

Fig. 09. Stratigraphic Section 1 located along the Candiota paleovalley (dip section in a N–S direction). It represents the gradual filling of the paleovalley, from south to north, by different sedimentary facies associations in the onlap of the crystalline basement of the Sul-Riograndense Shield and the Itararé Group of the Paraná Basin. The infilling started in the southern area, with development of a tide-dominated estuary at the base of Depositional Sequence 1. In the upper part of this sequence, a coastal barrier is developed in the south and the estuary changes from tide-dominated to a mixed-energy (tide-wave) condition. It is worth mentioning that arkosic sandstone predominates in the north valley (Stfmd and Stfw facies) and quartz rich sandstone in the south (Sttmd facies). In Depositional Sequence 2 the barrier-lagoon system is preserved, with costal barrier deposits in the south and back-barrier deposits in the north. In this sequence, lower shoreface and offshore-transition deposits are overlying the entire area. In this section, Depositional Sequence 1 and 2 are composed only by a transgressive system tract and boundary by subaerial unconformities (SB1 and SB2). The Supplementary Material presents the lithological profiles of the wells represented in this section (Fig. SM1).

and Stf facies). Overlying it, and across the entire paleovalley, estuarine sediments occur with important evidence of the tide action (Sttmd, Stfmd, Stfw, and Ht facies). In the upper part of Depositional Sequence 1, the progressive development of a coastal barrier (Shwf, Shw, and Stw facies) in the south is contemporaneous with the decreasing evidence of tidal deposition. Depositional Sequence 2 reveals a significant shift in factors controlling sediment deposition. Facies related to tidal action practically disappear, being replaced by the development of coastal barrier systems (Shwf, Shw, and Stw facies) and back-barrier facies (F, Fc, C, and Shwf). In the latter, there were conditions for the formation of important coal deposits (C facies). The sedimentation of sequence 2 throughout the region ends with the extensive development of offshore facies (Shcs, Hw, and rare Sm).

In Depositional Sequence 1, the estuarine facies corresponds to approximately 90% of the sedimentary record. In the lower part of this sequence there is a significant difference between the composition of the central and lower tidal-influenced estuary sandstone facies (Stfmd, Stfw, and Sttmd), allowing us to theorize over its genesis. The sediments of Stfmd and Stfw facies are poorly sorted, arkose, and frequently conglomeratic, indicating a proximal source area. On the other hand, sediments of the Sttmd facies are quartz-sandstone, well sorted, and with rounded grains, suggesting long-distance transport (McCubbin, 1982; Leuven et al., 2016, 2018). Sediments of Stfmd and Stfw facies are supplied by fluvial systems and reworked by tide currents as suggested by the presence of mud drapes and the sigmoidal erosion surfaces. This indicates that at this portion of the estuary, the flood tidal current was strong enough to produce reverse flow structures. The Sttmd facies sediment composition and texture are similar to the facies of the barrier (Shwf, Shw, Stw, and Sha), indicating they are likely longshore drift deposits, carried into the estuary by the flood tidal currents (McCubbin, 1982; Dalrymple et al., 1992; Leuven et al. 2016, 2018). Outcrops show that tidally influenced fluvial deposits (Stfmd and Stfw facies) have southward paleocurrents. For Sttmd facies there is no record of paleocurrents, however, the sediment texture and composition indicate the sediment is likely transported northward. All these characteristics suggest an estuary with two sources of sediment and the dominance of tidal currents, indicating the presence of a tide-dominated estuary (Dalrymple et al., 1992) (Fig. 13A and B).

Contemporaneous with the tide-dominated estuary, in the middle part of Depositional Sequence 1, there is the development of an incipient sandy barrier in the western side of the estuary mouth (Fig. 13B). In the upper part of this depositional sequence, the barrier system migrates eastward, but the inlet is wide and an important feature in the estuary (Fig. 13C). However, this barrier does not change the dominant processes in the inner estuary, where the tidal energy remains significant. The evidence is that fine-grained sediments of a central basin do not occur in the estuary. Therefore, the absence of facies in the central basin and bay-head delta, and the dominance of tidal deposits are compatible with mixed energy (tidal and wave) estuary (Boyd et al., 1992; Dalrymple et al., 1992, 2012, 2012; Dalrymple and Choi, 2007). Therefore, we can infer that the entire Depositional Sequence 1 corresponds to the evolution of a tidal to mixed-dominated estuary. It is important to mention that in this depositional sequence, in different parts of the estuary, relatively thick deposits of debris flow occur (Dm facies), indicating the presence of steep walls in the paleovalley.

Depositional Sequence 2 shows a significant change in the depositional environment, where the tide-dominated estuary of Depositional Sequence 1 is replaced by a wave-dominated coast (coastal barriers with

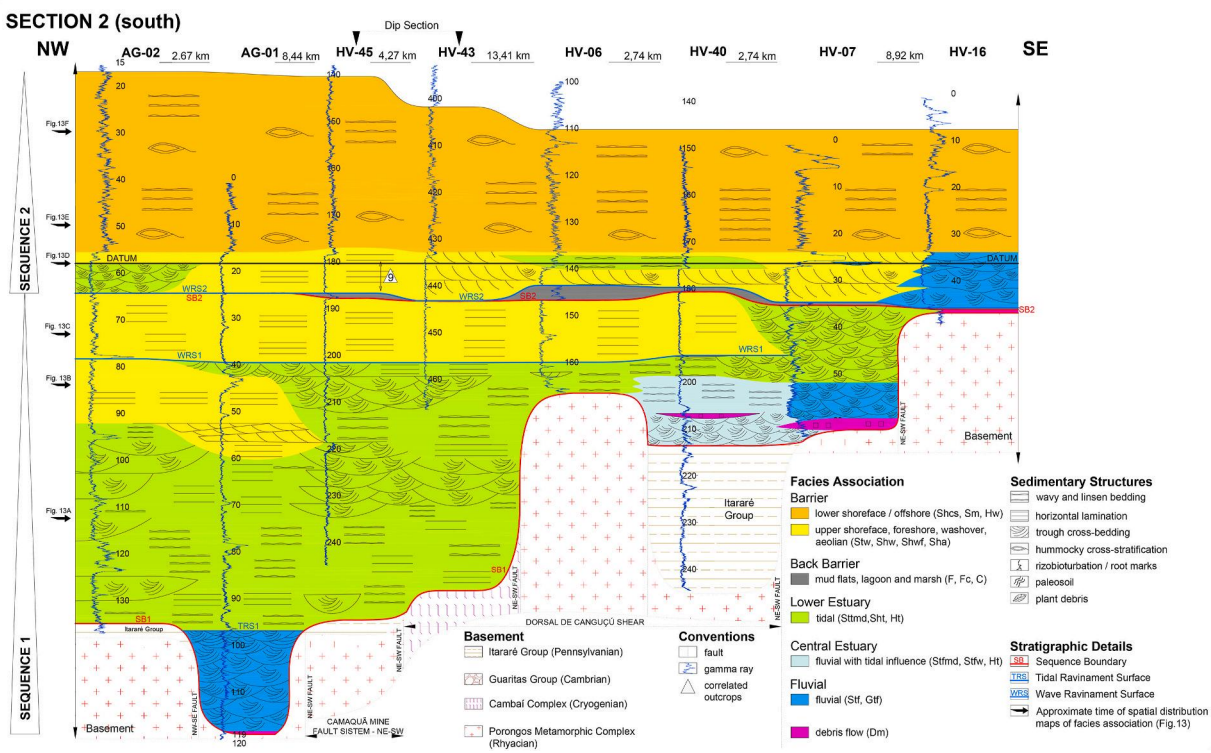

Fig. 10. Stratigraphic Section 2 - strike section in the southern area (NW-SE direction). In this section, basal infill of Depositional Sequence 1 is represented by fluvial facies association onlapping the basement. Overlying the fluvial deposits, the tide-dominated estuary is mostly composed of quartz-rich sandstone (Sttmd facies). In upper Depositional Sequence 1, the coastal barrier predominates, and the estuarine deposits only occur on the east side. Depositional Sequence 2 is predominantly formed by barrier deposits with lenticular beds of estuarine and fluvial deposits. It is important to mention that on the east side of this section there are two wedges of fluvial deposits, likely related to a fluvial system in a tributary valley. In Depositional Sequence 1, the contact between the basal fluvial and estuarine deposits records the Tidal Ravinement Surface (TRS1), only identified in this section, and the contact between the estuarine and barrier deposits records the Wave Ravinement Surface (WRS1). In Depositional Sequence 2, the Wave Ravinement Surface (WRS2) occurs in the contact between back-barrier and barrier deposits. The Supplementary Material presents the lithological profiles of the wells represented in this section (Fig. SM2).

associated lagoons and marshes). In the lower part of this sequence, the lagoon-barrier system is fully established in the southern area (Fig. 13D). Toward the upper sequence, the system migrates landward, and at the same time, the coal-bearing environments took place in the back-barrier plain (Fig. 13D and E). The upper part of this sequence is marked by offshore-transitional deposits, which are overlying most of the area. In the northeast, barrier and back-barrier systems still remain (Fig. 13F).

The sandy barrier of Depositional Sequence 2 is mainly composed of washover fans (Shwf), followed by foreshore (Shw), upper and lower shorefaces (Stw, Shcs, Hw, and Sm), and an aeolian sand sheet (Sha). The washover fan deposits preservation is common during transgressive events (Reinson, 1992; Nielsen and Nielsen, 2006). The back-barrier plain is formed by lagoon and swamp (F, Fc, and C) and isolated fluvial channels deposits (Stf).

Depositional models for the Candiota paleovalley area were previously described by Lavina and Lopes (1987), Alves and Ade (1996), Holz (2003), and Trentin et al. (2019). The studies performed by Alves and Ade (1996) and Holz (2003) describe the basal infill of the valley along the entire N–S axis as composed by coarse-grained arkosic sandstones, interpreted as different subsystems (distributary channel, interdistributary bay, proximal, distal and very distal distributary mouth bar, and prodelta) of a fluvial-deltaic system. Restricted to a paleohills neighborhood, local alluvial fan deposits were identified by Holz (2003), Oliveira and Kalkreuth (2010). Overlying the fluvial facies, in the distal portion of the valley, Holz (2003) describes fine-grained clean sandstone and mudstone representing the development of small barriers isolating a lagoonal estuary with a central bay and bayhead delta zones. The lagoonal estuary depositional environment is also described by Oliveira and Kalkreuth (2010). Both authors attribute this environment to the genesis of the main Candiota coal beds. In the upper part, of the model by Holz (2003) the barrier-lagoon system migrates landward, overlying the lagoonal estuary.

Previous depositional models have similarities and differences in comparison to the model presented here. In our interpretation, the basal sedimentary facies are composed of arkosic sediments representing fluvial deposits reworked by tidal current through the entire valley. Tidal diagnostic structures are characteristics of this interval; moreover, Fritzen et al. (2019) have identified tidal neap-spring cyclicity in outcrop corroborating the energy of the tidal current within the inner part of the estuary. Therefore, besides local fluvial deposits in the deepest and distal part of the valley, this sediment deposition already occurred in a tidal-dominated estuary. The hetherolith facies interpreted by Holz (2003) as interdistributary bays, very distal mouth bar, and prodelta, in this study they are related to the estuary. Heterolith facies with bioturbated indexes between 1 and 3 were interpreted as mixed flat, while intense bioturbated heterolith, with indexes between 4 and 6, are lower shoreface deposits in the context of the lower estuary. Another difference is related to the coal-forming environment, in our model it is attributed to the back-barrier plain, in a wave-dominated coast formed after the entire infill of the paleovalley, instead of a lagoonal estuary. Lavina and Lopes (1987), Alves and Ade (1996), and Trentin et al. (2019) have also interpreted a back-barrier plain environment for the genesis of the Candiota coal measures.

The tide-dominated estuary of Depositional Sequence 1 was controlled by tidal amplification within the valley (see Fig. 2), reaching meso- to macro-tidal ranges according to scenarios presented by Candido et al. (2020). On the other hand, the barrier-lagoon system of

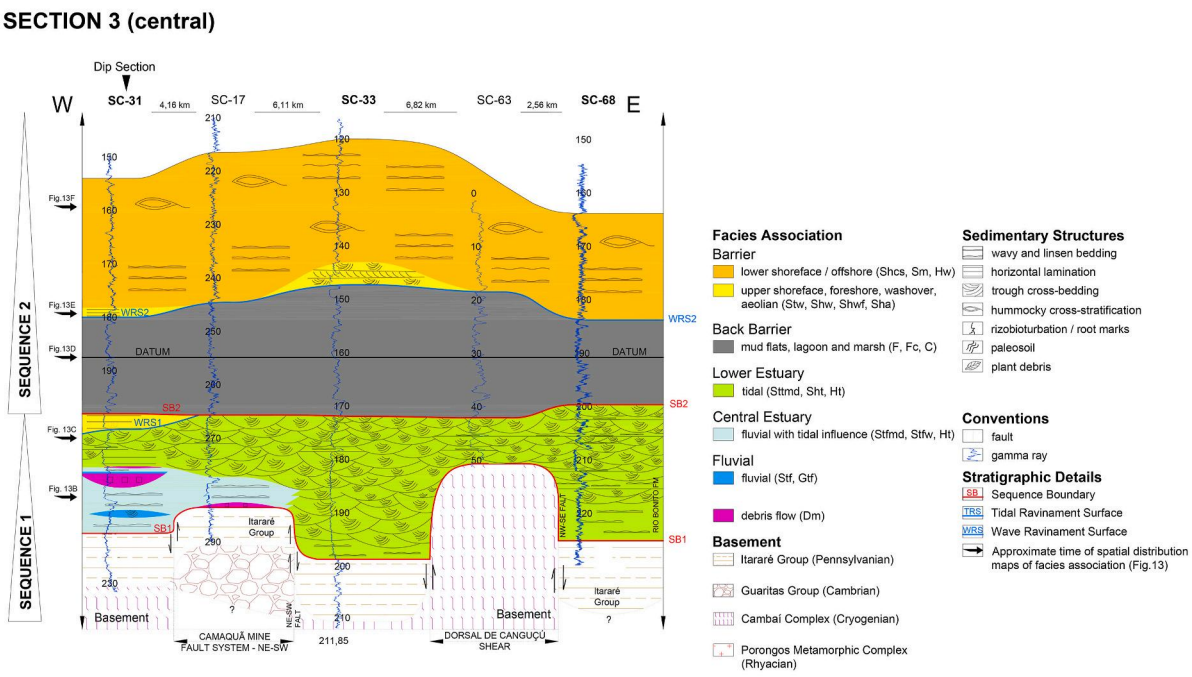

Fig. 11. Stratigraphic Section 3 - strike in the central area (E-W direction). Depositional Sequence 1 is predominantly represented by lower estuary deposits (Sttmd and Ht facies), while central estuary deposits (Stfmd facies and Ht) are restricted to the west side of the paleovalley with subordinate fluvial deposits (Stf) and debris flow deposits (Dm facies). Barrier deposits occur locally at the top of Depositional Sequence 1, on the west side. In Depositional Sequence 2, back-barrier deposits (F, Fc, and C facies) are predominant in the lower part, and the barrier is overlying them. The barrier deposits are mainly composed of lower shoreface facies. The contact between back barrier and barrier facies association records the Wave Ravinement Surface (WRS2). The Supplementary Material presents the lithological profiles of the wells represented in this section (Fig. SM3).

Depositional Sequence 2 represents a moment of tectonic stability, where subsidence rates were low, and a microtidal regime was established (Lavina and Lopes, 1987; Lopes et al., 2003a). Therefore, from the base to the top of the succession, there is a significant decrease in the tidal range regime. The depositional system evolution in Depositional Sequence 1 which shows a transition from tidal-to mixed-energy estuary, corroborates this interpretation.

The tide-dominated estuary occurs within the funnel-shaped valley, in which the morphology controls the tidal amplification (Flemming, 2011; Longhitano et al., 2012). The development of a mixed-energy estuary might have been promoted by a high to moderate wave energy associated with the meso-to macro-tidal range and high volume of marine sediment available (Tessier, 2012). In contrast, the barrier-lagoon system was formed along a linear coast, after the complete infilling of the valley. Thus, we associate the variation in the tidal range with the evolution of the relief and infill of the valley (Dalrymple and Choi, 2007; Longhitano et al., 2012; Tessier, 2012; Dalrymple and Padman, 2017). The infill of the estuary attenuates the relief, causing the decrease in tidal prism (Pendón et al., 1998). In the context of a small tidal prism, the wave energy became dominant, allowing the development of linear coasts and barrier systems (Boyd et al., 1992; Dalrymple et al., 1992; Johnson and Baldwin, 1996; Péndon et al., 1998; Ainsworth et al., 2011).

Tidal-dominated estuaries are common depositional environments formed during interglacial and post-glacial periods when the sea-level rise controlled by deglaciation floods formed incised valleys (e.g., Hori et al., 2001; Lin et al., 2005; Tjallingii et al., 2010). On the southwestern coast of Spain, the Flandrian transgression (Holocene) flooded incised valleys forming tidal-dominated estuaries (Borrego et al., 1995; Péndon et al., 1998; Dabrio et al., 2000), and some of them have evolved to wave-dominated estuaries because of the rapid infill and progressive decrease in tidal prism (Borrego et al., 1995; Péndon et al., 1998). Three successive stages of evolution were described for by Péndon et al. (1998): a tide-dominated open stage with strong tidal currents; a wave-dominated period, in which waves introduced sand into the inner estuary, forming sandy bodies and barriers; and, a second tide-dominated stage with weaker tidal currents, before the estuary finally filled. The Holocene tidal-to wave-dominated coast transition is well described along the coast of Spain but scarce in ancient records. Therefore, we show a Permian case study that can improve the understanding of the progressive transition from a tidal-dominated estuary to a mixed-energy estuary caused by the development of a coastal barrier during a transgression period.

6. Conclusions

The early Permian sedimentation in the southern Paraná Basin provided insights of a significant change in the process controlling the sediment transport and deposition, influenced by the coastline morphology. Sedimentation starts within a funnel-shaped valley, promoting tidal amplification and a tide-dominated estuary development during transgression. Throughout the valley infill, estuarine conditions changed, and an incipient distal barrier started developing. At this time, a mixed-energy estuary was established. In the upper part, after the

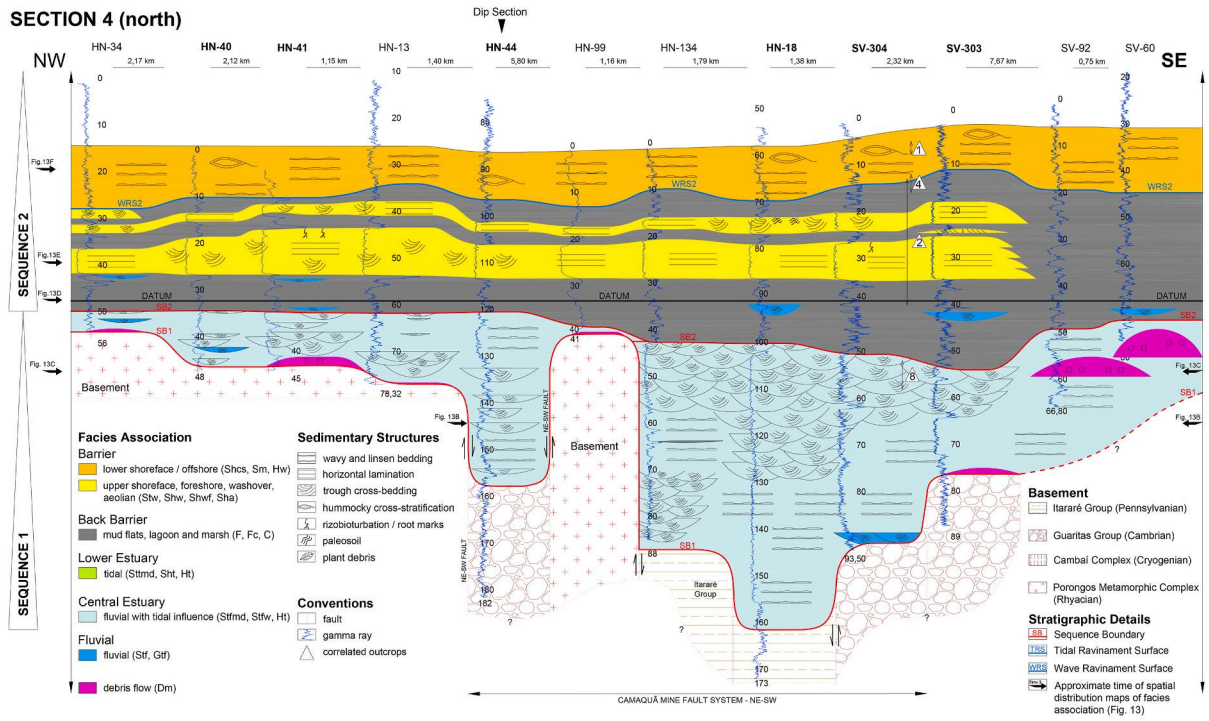

Fig. 12. Stratigraphic Section 4 - strike section in the north area (NW-SE direction). Depositional Sequence 1 is predominantly represented by central estuary deposits (Stfmd and Ht facies), with fluvial (Stf and Gtf facies) and debris flow deposits (Dm facies) interbedded locally. In Depositional Sequence 2, back-barrier deposits (F, Fc, C, Shwf, and Stf facies) are predominant in the lower part. Lenticular beds of horizontal lamination quartz-rich sandstone of the Shwf facies, representing storm deposits (washover fan), occur interbedded with fine-grained facies of the back-barrier deposits. The Wave Ravinement Surface (WRS2) records the contact of the barrier (Shcs and Hw facies) with the back-barrier facies. The Supplementary Material presents the lithological profiles of the wells represented in this section (Fig. SM4).

complete infill of the paleovalley, an extensive coastal system was formed due to the tidal prism decrease, promoting the coastal barrier system formation.

The tide-dominated lower estuary was developed over basal fluvial deposits. In the central estuary, tidal flats and tidal bars are composed of poor sorted arkose sediments supplied by fluvial systems. In the same way, the lower estuary is also formed by tidal flats and tidal bars, but there is a remarkable change in the sediment composition of the tidal bar deposits. In the lower estuary, sandstone is fine-grained, well sorted, and quartz-rich, suggesting a distinct source. These sediments were supplied by littoral drift and transported along the inner estuary by flood tidal currents. The presence of two sediment sources, proximal (fluvial) and distal (littoral drift), remain along the mixed-energy estuary development.

The coastal barrier system in the upper part is composed of quartz-rich fine-to medium-sandstones, developing first in the southwest and progressively migrating towards the northeast. In the widespread back-barrier plain, conditions favored the peat accumulation and further the important coal measure formation. By the end of the succession, the coastal barrier system formed in the northeast and the entire south area was under offshore condition.

Therefore, a tidal- and mixed-energy estuarine system developed (Depositional Sequence 1) and later, a barrier-lagoon system, in which thick and extensive coal layers were generated (Depositional Sequence 2). The morphology of the paleovalley was fundamental in the tidal range amplification, and after the complete infill of the valley, the development of a linear coast is in agreement with the dominance of a microtidal regime in the upper part of the section, where wave energy was predominant. The inner morphology of the paleovalley reinforces the conclusion that a sinuous funnel-shaped valley favors the tidal range amplification.

Author agreement statement

We the undersigned declare that this manuscript is original, has not been published before and is not currently being considered for publication elsewhere. We confirm that the manuscript has been read and approved by all named authors and that there are no other persons who satisfied the criteria for authorship but are not listed. We further confirm that the order of authors listed in the manuscript has been approved by all of us. We understand that the Corresponding Author is the sole contact for the Editorial process. He/she is responsible for communicating with the other authors about progress, submissions of revisions and final approval of proofs.

Authorship contributions

Conception and design of study: Lavina, E. L. C. Acquisition of data: Lavina, E. L. C., Galli, C. P., Cagliari, J. Analysis and/or interpretation of data: Lavina, E. L. C., Galli, C. P. Drafting the manuscript: Galli, C. P. Revising the manuscript critically for important intellectual content: Lavina, E. L. C., Cagliari, J. Approval of the version of the manuscript to be published (the names of all authors must be listed): Lavina, E. L. C., Galli, C. P., Cagliari, J.

Declaration of competing interest

The authors declare that they have no known competing financial interests or personal relationships that could have appeared to influence the work reported in this paper.

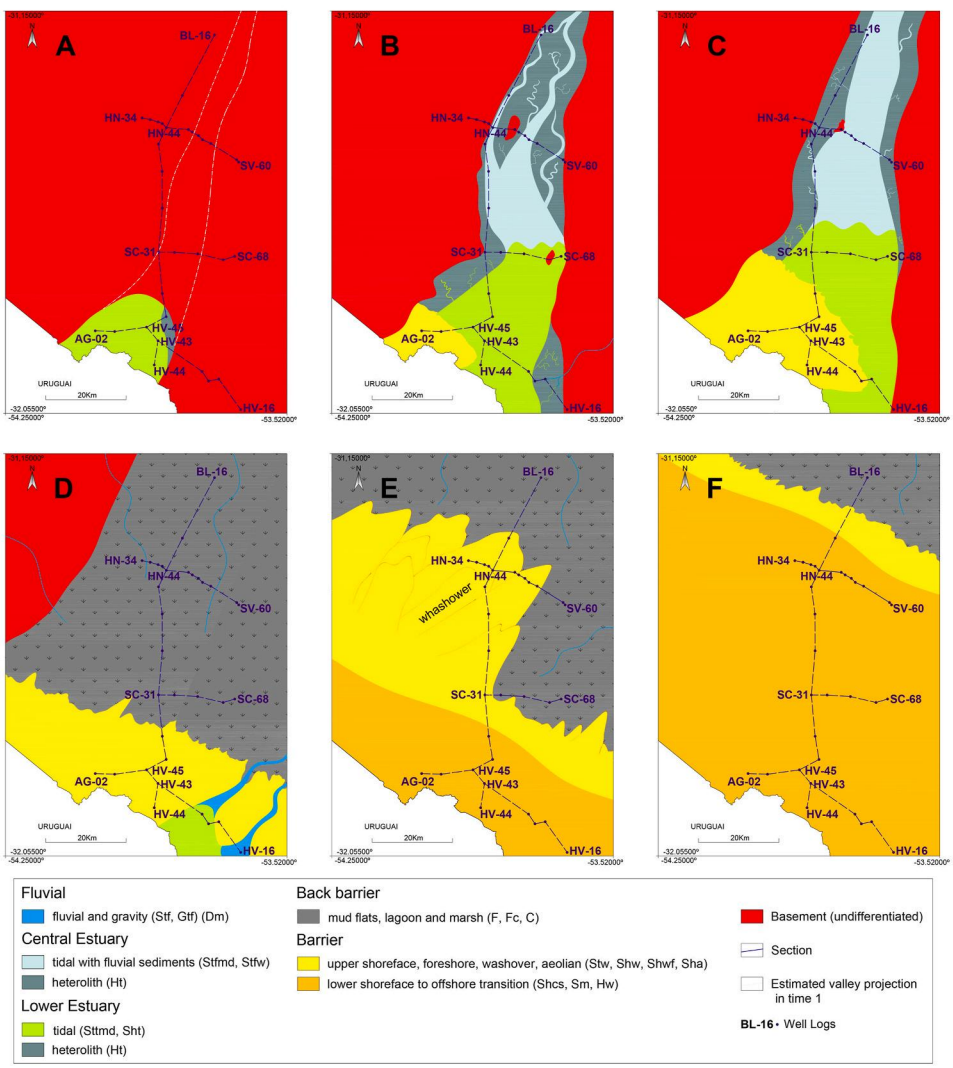

Fig. 13. Paleogeographic evolution maps of the studied area. A-C) Depositional Sequence 1 - progressive infill of the paleovalley showing facies association distribution in the estuarine system. D-F) Depositional Sequence 2 – Coastal system evolution showing the progressive landward migration of the barrier system over the lagoon and swamp deposits. A) Initial sedimentary infill of the paleovalley in the southern area by the formation of a tide-dominated estuary. B) Development of the tide-dominated estuary along the paleovalley with the incipient barrier formation in the southwest. C) Barrier system migration toward the southeast and the estuary energy changed from tide-to tide-wave-dominated. D) Formation of a linear coastal system (SE-NW direction) protecting an extensive back-barrier area with the development of the lagoon and swamp environment. E) Landward migration of the barrier system over the lagoon and swamp environments. Whashover fans predominate in the barrier system and mark the barrier destruction during storm events. Lower shoreface deposits represent the distal part of the barrier. F) Barrier system migration northward and the lower shoreface and offshore-transitional facies predominate in most of the area. Back-barrier environments only occur in the northeast.

Acknowledgements

This study was financed in part by the Coordenação de Aperfeiçoamento de Pessoal de Nível Superior – Brasil (CAPES) – Financial Code 001. The authors would like to thank CNPq for the grants provided for this study, which is linked to the project "Arquitetura Estratigráfica de Corpos Arenosos Gerados pela Interação entre Ondas e Correntes de Maré" (CNPq Edital Universal, process: 485495/2007-0), and the support of Unisinos for the project "Análise da história deposicional na borda sul da Bacia do Paraná no intervalo Neocarbonífero-Eopermiano". We give thanks to the Brazilian Geological Service (CPRM) for allowing access to the drill cores used in this paper. We also thank Dr. Claiton M. S. Scherer and the other reviewer for their significant contributions towards the improvement of this paper.

Appendix A. Supplementary data

Supplementary data to this article can be found online at https://doi.org/10.1016/j.jsames.2021.103398.

References

Aboarrage, A.M., Lopes, R.C., 1986. Projeto A Borda Leste da Bacia do Paraná: integração geológica e avaliação econômica. Relatório Final. DNPM/CPRM: Porto Alegre.

Ainsworth, R.B., Vakarelov, B.K., Nanson, R.A., 2011. Dynamic spatial and temporal prediction of changes in depositional processes on clastic shorelines: toward improved subsurface uncertainty reduction and management. AAPG (Am. Assoc. Pet. Geol.) Bull. 95, 267–297.

Alves, R.G., Ade, M.V.B., 1996. Sequence and coal petrography applied to the Candiota Field, Rio Grande do Sul, Brazil: a depositional model. Int. J. Coal Geol. 30, 231–248.

Anthony, E.J., Aagaard, T., 2020. The lower shoreface: morphodynamics and sediment connectivity with the upper shoreface and beach. Earth Sci. Rev. 210, 103334.

Bann, K.L., Fielding, C.R., MacEachern, J.A., Tye, S.C., 2014. Differentiation of Esturine and Offshore Marine Deposits Using Integrated Ichnology and Sedimentology: Permian Pebbley Beach Formation, vol. 288. Geological Society, London, Special Publications, Sydney Basin, Australia, pp. 179–211.

Best, J., Fielding, C.R., 2019. Describing fluvial systems: linking processes to deposits and stratigraphy. Geol. Soc. Londn. Special Public. 488, 152–166.

Boggs, S., 2006. Principles of Sedimentary and Stratigraphy. Pearson Prentice Hall.

Borrego, J., Morales, J.A., Pendon, J.G., 1995. Holocene estuarine facies along the mesotidal coast of Huelva, south-western Spain. Special Publ. Int. Assoc. Sedimentol. 24, 151–170.

Boyd, R., Dalrymple, R., Zaitlin, B.A., 1992. Classification of clastic coastal depositional environments. Sediment. Geol. 80, 139–150.

Boyd, R., Dalrymple, R.W., Zaitlin, B.A., 2006. Estuarine and incised valley facies models. In: Posamentier, H.W., Walker, R.G. (Eds.), Facies Models Revisited, vol. 84. SEPM Special Publication, pp. 171–235.

Buatois, L.A., Netto, R.G., Mangano, M.G., 2007. Ichnology of permian marginal – to shallow-marine coal-bearing successions: Rio Bonito and Palermo formations, Paraná Basin, Brazil. Palios 20, 321–347.

Cagliari, J., Lavina, E.L.C., Philipp, R.P., Tognoli, F.M.W., Basei, M.A.S., Faccini, U.F., 2014. New Sakmarian ages for the Rio Bonito formation (Paraná Basin, southern Brazil) based on LA-ICP-MS U-Pb radiometric dating of zircons crystals. J. S. Am. Earth Sci. 56, 265–277.

Cagliari, J., Philipp, R.P., Buso, V.V., Netto, R.G., Hillebrand, P.K., Lopes, R.C., Basei, M. A.S., Faccini, U.F., 2016. Age constraints of the glaciation in the Paraná Basin: evidence from new U-Pb dates. J. Geol. Soc. 173 (6), 871–875.

Candido, M., Cagliari, J., Tognoli, F.M.W., Lavina, E.L.C., 2019. Stratigraphic modeling of a transgressive barrier-lagoon in the Permian of Paraná Basin, southern Brazil. J. S. Am. Earth Sci. 90, 377–391.
Candido, M., Cagliari, J., Lavina, E.L.C., 2020. Tidal circulation in an Permian epicontinental sea: evidence of an amphidromic system. Paleogeogr. Paleoclimatol. Paleoecol. 546, 109671, 2020.
Casshyap, S.M., 1970. Sedimentary cycles and environment of deposition of the Barakar coal measures of lower Gondwana, India. J. Sediment. Res. 40 (4), 1302–1317.
Catuneanu, O., Abreu, V., Bhattacharya, J.P., Blum, M.D., Dalrymple, R.W., Eriksson, P. G., Fielding, C.R., Fisher, W.L., Galloway, W.E., Gibling, M.R., Giles, K.A., Holbrook, J.M., Jordan, R., Kendall, C.G. St C., Macurda, B., Martinsen, O.J., Miall, A.D., Neal, J.E., Nummedal, D., Pmar, L., Posamntier, H.W., Pratt, B.R., Sarg, J.F., Shanley, K.W., Steel, R.J., Strasser, A., Tucker, M.E., Winker, C., 2009. Towards the standardization of sequence stratigraphy. Earth Sci. Rev. 92, 1–33.
Catuneanu, O., Galloway, W.E., Kendall, C.G. St C., Miall, A.D., Posamentier, H.W., Strasser, A., Tucker, M.E., 2011. Sequence stratigraphy: methodology and nomenclature. Newsl. Stratigr. 44/3, 173–245.
Cheel, R.J., Leckie, D.A., 1993. Hummocky cross-stratification. Sedimentol. Rev. 1, 103–122.
Clemmensen, L.B., Surlyk, F., 1976. Upper Jurassic coal-bearing shoreline deposits, Hochstetter Forland, east Greenland. Sediment. Geol. 15 (3), 193–211.
Clifton, H.E., 1976. Wave-formed sedimentary structures – a conceptual model. In: Davis, R.A., Ethington, R.L. (Eds.), Beach and Nearshore Sedimentation, vol. 24. SEPM Special Publication, pp. 126–148.
Clifton, H.E., 2006. A re-examination of facies models for clastic shorelines. In: Posamentier, H.W., Walker, R.G. (Eds.), Facies Models Revisited, vol. 84. Society for Sedimentary Geology (SEPM) Special Publication, pp. 293–337.
Collinson, J.D., 1970. Bedforms of the tana river, Norway. Geogr. Ann. Phys. Geogr. 52 (1), 31–56.
Collinson, J.D., 1996. Alluvial sediments. In: Reading, H.G. (Ed.), Sedimentary Environments: Process, Facies and Stratigraphy. Blackwell Scientific Publications, Oxford, pp. 37–82.
Collinson, J., Mountney, N., Thompson, D., 2006. Sedimentary Structures. Terra Publishing, England, p. 292.
Cristino, J., Dabrio, C.J., Zazo, C., Goy, J.L., Sierro, F.J., Borja, F., Lario, J., González, J. A., Flores, J.A., 2000. Depositional history of estuarine infill during the last postglacial transgression (Gulf of Cadiz, Southern Spain). Mar. Geol. 162, 381–404.
Daidu, F., 2013. Classifications, sedimentary features and facies associations of tidal f lats. J. Palaeogeogr. 2 (1), 66–80.
Dalrymple, R.W., Choi, K., 2007. Morphologic and faceis trends through the fluvial-marine transition in tide-dominated depositional systems: a schematic framework for environmental and sequence-stratigraphic interpretation. Earth Sci. Rev. 81, 135–174.
Dalrymple, R.W., Padman, L., 2017. Are Tides Controlled by Latitude? Society for Sedimentary Geology, vol. 108. Special Publication, pp. 1–17.
Dalrymple, R.W., Zaitlin, B.A., Boyd, R., 1992. Estuarine facies models: conceptual basis and stratigraphic implications. J. Sediment. Petrol. 62 (6), 1130–1146.
Dalrymple, R.W., Mackay, D.A., Ichaso, A.A., Choi, K.S., 2012. Processes, morphodynamics, and facies of tide-dominated estuaries. In: Davis, R.A., Dalrymple, R.W. (Eds.), Principles of Tidal Sedimentology. Springer Science+ Business Media B, Dordrecht, pp. 79–107.
Davis, R.A., Clifton, H.E., 1987. Sea-level Change and the Preservation Potential of Wave-Dominated and Tide-Dominated Coastal Sequences, vol. 41. The Society of Economic Paleontologists and Mineralogists Special Publication, pp. 167–178.
De Boer, P.L., Oost, A.P., Visser, M.J., 1989. The diurnal inequality of the tide as a parameter for recognizing tidal influences. J. Sediment. Res. 59, 912–921.
Desjardins, P.R., Buatois, L.A., Mángano, M.G., 2012. Tidal flats and subtidal sand bodies. In: Trace Fossils as Indicators of Sedimantary Environments, vol. 64, pp. 529–561.
Dumas, S., Arnott, R.W.C., 2006. Origin of hummocky and swaley cross-stratification - the controlling influence of unidirectional current strength and aggradation rate. Geology 34 (12), 1073–1076.
Elliott, T., 1986. Clastic shorelines. In: Reading, H.G. (Ed.), Sedimentary Environments and Facies. Blackwell Scientific Publications, Oxford, pp. 143–177.
Eyles, N., Kocsis, S., 1988. Sedimentology and clast fabric of subaerial debris flow facies in a glacially-influenced alluvial fan. Sediment. Geol. 59, 15–28.
Flemming, B.W., 2011. Geology, morphology and sedimentology of estuaries and coasts. In: Flemming, B.W., Hansom, J.D. (Eds.), Treatise on Estuaries and Coasts, Volume 3, Estuarine and Coastal Geology and Morphology. Elsevier, Amsterdam, pp. 7–38.
Flemming, B.W., 2012. Siliciclastic back-barrier tidal flats. In: Davis Jr, R.A., Dalrymple, R.W. (Eds.), Principles of Tidal Sedimentology. Springer, Dordrecht, pp. 231–267.
Flores, R.M., 1978. Coal depositional models in some Tertiary and Cretaceous coal fields in the U.S. Western Interior. U.S.Geol. Surv. I, 225–235.
Fritzen, M.R., Cagliari, J., Candido, M., Lavina, E.L.C., 2019. Tidal bar cyclicity in the lower permian: the Rio Bonito Formation, Paraná Basin, southern Brazil. Sediment. Geol. 381, 76–83.
Gandini, R., Netto, R.G., Kern, H.P., Lavina, E.L.C., 2010. Assinaturas icnológicas da sucessão sedimentar Rio Bonito no bloco central da jazida carbonífera de Iruí, Cachoeira do Sul (RS). GAEA J. Geosci. 6 (1), 21–43.
Greenwood, B., 2006. Bimodal cross-lamination in wave-ripple form sets: a possible origin. J. Coast Res. 22 (5), 1220–1229.
Griffis, N.P., Mundil, R., Montañez, I.P., Isbell, J., Fedorchuck, N., Vesely, F., Iannuzzi, R., Yin, Q.S., 2018. A new stratigraphic framework built on U-Pb singlezircon TIMS ages and implications for the timing of the penultimate icehouse (Paraná Basin, Brazil). Geol. Soc. Am. Bull. 130, 848–858.
Harms, J.C., Southard, J.B., Walker, R.G., 1982. Structures and sequences in clastic rocks. 737 SEPM Short Course Notes 9.
Heward, A.P., 1981. A review of wave-dominated clastic shoreline deposits. Earth Sci. Rev. 17, 223–276.
Holz, M., 1999. Early Permian sequence stratigraphy and the palaeophysiographic evolution of the Paranti Basin in southernmost Brazil. J. Afr. Earth Sci. 29, 51–61.
Holz, M., 2003. Sequence stratigraphy of a lagoonal estuarine system – an example from the lower permian Rio Bonito Formation. Paraná Basin, Brazil: Sediment. Geol. 162, 305–331.
Holz, M., França, A.F., Souza, P.A., Iannuzzi, R., Rohn, R., 2010. A stratigraphic chart of the Late Carboniferous/Permian succession of the eastern border of the Paraná Basin, Brazil, South America. J. South Am. Earth Sci. 29 (2), 381–399.
Holz, M., Küchle, J., Philipp, R.P., Bischoff, A.P., Arima, N., 2006. Hierarchy of tectonic control on stratigraphic signatures: base-level changes during the Early Permian in the Parana Basin, southernmost Brazil. J. S. Am. Earth Sci. 22, 185–204.
Hori, K., Saito, Y., Zhao, Q., Cheng, X., Wang, P., Sato, Y., Li, C., 2001. Sedimentary facies of the tide-dominated paleo-Changjiang (Yangtze) estuary during the last transgression. Mar. Geol. 177, 331–351.
Iverson, R.M., 1997. The physics of debris flows. Rev. Geophys. 35 (3), 245–296.
Iverson, R.M., 2009. Elements of an improved model of debris-flow motion. In: Nakagawa, M., Luding, S. (Eds.), Proceedings of the Sixth International Conference on Micro-mechanics of Granular Media. American Institute of Physics, pp. 9–16.
Jasper, A., Menegat, R., Sommer, M.G., Klepzig, M.C., Souza, P.A., 2006. Depositional cyclicity and paleoecological variability in an outcrop of Rio Bonito Formation, early perminal, Paraná Basin, Rio Grande do sul, Brazil. South Am. Earth Sci. 21, 276–293.
Johnson, H.D., Baldwin, C.T., 1996. Shallow clastic seas. In: Reading, H.G. (Ed.), Sedimentary Environments: Process, Facies and Stratigraphy. Blackwell Scientific Publications, Oxford, pp. 232–280.
Kocurek, G., 1991. Interpretation of ancient eolian sand dunes. Annu. Rev. Earth Planet Sci. 19, 43–75.
Kocurek, G., Dott, R.H., 1981. Distinctions and uses of stratification types in the interpretation of eolian sand. J. Sediment. Petrol. 51, 579–595.
Kocurek, G., Nielson, J., 1986. Condition favourable for the formation of warm-climate aeolian sand sheets. Sedimentology 33, 795–816.
Lancaster, N., 1995. Geomorphology of Desert Dunes. Routledge Physical Environment Series, p. 312p.
Lavina, E.L.C., Lopes, R.C., 1987. A transgressão marinha do Permiano Inferior e a evolução paleogeográfica do Supergrupo Tubarão no Estado do Rio Grande do Sul. Paula-Coutina 1, 51–103.
Lavina, E.L.C., Nowatzki, C.H., Santos, M.A.A., Leão, H.Z., 1985. Ambientes de Sedimentação do supergrupo tubarão na região de Cachoeira do sul, RS. Acta Geol. Leopoldensia 9, 5–75.
Le Hir, P., Cayocca, F., Waeles, B., 2011. Dynamics of sand and mud mixtures: a multiprocess-based modelling strategy. Continent. Shelf Res. 31 (10), S135–S149.
Leckie, D.A., Walker, R.G., 1982. Storm- and tide-dominated shorelines in Cretaceous Moosebar-Lower Gates interval- Outcrop equivalents of deep basin gas trap in Western Canada. Bull. Am. Assoc. Pet. Geol. 66, 138–157.
Leuven, J.R.F.W., Kleinhans, M.G., Weisscher, S.A.H., van der Vegt, M., 2016. Tidal sand bar dimensions and shapes in estuaries. Earth Sci. Rev. 161, 204–223.
Leuven, J.R.F.W., van Maanen, B., Lexmond, B.R., van der Hoek, B., Spruijt, M.J., Kleinhans, M.G., 2018. Dimensions of fluvial-tidal meanders: are they disproportionally large? Geology 46 (10), 923–926.
Li, M.Z., Amos, C.L., 1999. Sheet flow and large wave ripples under combined waves and currents: field observations, model predictions and effects on boundary layer dynamics. Continent. Shelf Res. 19, 637–663.
Lin, C., Zhuo, H., Gao, S., 2005. Sedimentary facies and evolution in the Qiantang River incised valley, eastern China. Mar. Geol. 219, 235–259.
Longhitano, S.G., Mellere, D., Steel, R.J., Ainsworth, R.B., 2012. Tidal depositional systems in the rock record: a review and new insights. Sediment. Geol. 279, 2–22.
Lopes, R.C., 1995. Arcabouço aloestratigráfico para o intervalo "Rio Bonito-Palermo" (Eopermiano da Bacia do Paraná), entre Butiá e São Sepé, Rio Grande do Sul. Dissertação de Mestrado, Centro de Ciências Exatas e Tecnológicas, Universidade do Vale do Rio dos Sinos, p. 245.
Lopes, R.C., 2004. Arquitetura deposicional e potential de armazenamento em arenitos associados às jazidas de carvão da Formação Rio Bonito na região do Rio Jacuí, Rio Grande do Sul. Tese de Doutorado, Centro de Ciências Exatas e Tecnológicas, Universidade do Vale do Rio dos Sinos, p. 303.
Lopes, R.C., Lavina, E.L., 2001. Estratigrafia de Sequências nas Formações Rio Bonito e Palermo (Bacia do Paraná), na região carbonífera do Jacuí, Rio Grande do Sul. In: Ribeiro, H.J.P.S. (Ed.), Estratigrafia de sequências: fundamentos e aplicações, Universidade do Vale do Rio dos Sinos – UNISINOS, pp. 391–419.
Lopes, R.C., Lavina, E.L., Paim, P.S.G., Goldberg, K., 2003a. Controle Estratigráfico e Deposicional na Gênese dos Carvões da Região do Rio Jacuí (RS). In: Paim, P.S.G., Faccini, U.F., Netto, R.G. (Eds.), Geometria Arquitetura e Heterogeneidade de corpos sedimentares – Estudos de Casos, Universidade do Vale do Rio dos Sinos – UNISINOS, pp. 187–206.
Lopes, R.C., Paim, P.S.G., Lavina, E.L., 2003b. Modelo de Reservatório em arenitos litorâneos: ilha de Barreira permiana na formação Rio Bonito (minas do leão-RS). In: Paim, P.S.G., Faccini, U.F., Netto, R.G. (Eds.), Geometria Arquitetura e Heterogeneidade de corpos sedimentares – Estudos de Casos, Universidade do Vale do Rio dos Sinos – UNISINOS, pp. 187–206.
Maahs, R., Küchle, J., Scherer, C.M.S., Alvarenga, R.S., 2019. Sequence stratigraphy of fluvial to shallow-marine deposits: the case of the early Permian Rio Bonito Formation, Paraná Basin, southernmost Brazil. Braz. J. Genet. 49, e20190059.

MacEachern, J.A., Pemberton, S.G., Gingras, M.K., Bann, K.L., 2010. Ichnology and facies models. In: James, N.P., Dalrymple, R.W. (Eds.), Facies Models 4. Geological Association of Canada, pp. 19–58.
Mángano, M.G., Buatois, L.A., 2014. Ichnology of Carboniferous tide-influenced environments and tidal flat variability in the North American Midcontinent., 2014. In: McIlroy, D. (Ed.), The Apllication of Ichnology to Palaeonvironmental and Stratigraphic Analysis, vol. 228. Geological Society, London, Special Publications, pp. 157–178.
Masselink, G., Puleo, J.A., 2006. Swash-zone morphodynamics. Continent. Shelf Res. 26, 661–680.
McCabe, P.J., 1985. Depositional environments of coal and coal-bearing strata. In: Rahmani, R.A., Flores, R.M. (Eds.), Sedimentology of Coal and Coal-Bearing Sequences. Special Publication of the International Association of Sedimentologists, pp. 13–42.
McCubbin, D.G., 1982. Barrier-island and strand-plain facies. In: Scholleand, P.A., Spearing, D.R. (Eds.), Sandstone Depositional Environments, vol. 31. AAPG Memoir, pp. 247–280.
Miall, A.D., 1977. A review of the braided-river depositional environments. Earth Sci. Rev. 13, 1–62.
Miall, A.D., 2006. The Geology of Fluvial Deposits - Sedimentary Facies, Basin Analysis, and Petroleum Geology. Springer, p. 589.
Milani, E.J., Faccini, U.F., Scherer, C.M., Araújo, L.M., Cupertino, J.A., 1998. Sequence and stratigraphic hierarchy of the Paraná Basin (ordovician to cretaceous), southern Brazil. Boletim IG USP (Sér. Sci.) 29, 125–173.
Milani, E.J., Melo, J.H.G., Souza, P.A., Fernandes, L.A., França, A.B., 2007. Bacia do Paraná. Boletim de Geociências da PETROBRÁS. Rio de Janeiro 15 (2), 265–287.
Mottin, T.E., Vesely, F.F., Rodrigues, M.C.N.L., Kipper, F., Souza, P.A., 2018. The paths and timing of Late Paleozoic ice Revisited: new stratigraphic and paleo-ice flow interpretations from glacial sucession in the upper Itararé Group (Paraná Basin, Brazil). Palaeogeogr. Palaeoclimatol. Paleoecol. 490, 488–504.
Myrow, P., Southard, J., 1991. Combined-flow model for vertical stratification sequences in shallow marine storm-deposited beds. J. Sediment. Res. 61 (2), 202–210.
Nielsen, N., Nielsen, J., 2006. Development of a washower fan on a transgressive barrier, skallingen dnmark. J. Coast Res. 39, 207-111.
Oliveira, J.S., Kalkreuth, W., 2010. Sequence stratigraphy, organic petrology and chemistry applied to the upper and lower coal seams in the Candiota Coalfield, Paraná Basin, RS, Brazil. Int. J. Coal Geol. 84, 258–268.
Pemberton, S.G., MacEachern, J.A., Dashtgard, S.E., Bann, K.L., Gingras, M.K., Zonneveld, J.P., 2012. Chapter 19 - shorefaces. Dev. Sedimentol. 64, 563–603.
Pendón, J.G., Morales, J.A., Borrego, J., Jimenez, I., Lopez, M., 1998. Evolution of estuarine faceis in a tidal channel environment SW Spain: evidence for a change from tide-to wave-domination. Mar. Geol. 147, 43–62.
Pyrcz, M.J., 2015. A Review of Some Fluvial Styles, Research Gate, Publication 237713953.
Raaf, J.F.M., Boersma, J.R., Gelder, A., 1977. Wave-generated structures and sequences from a shallow marine succession, Lower Carboniferous, County Cork, Ireland. Sedimentology 24 (4), 451–483.
Reading, H.G., Collinson, J.D., 1996. Clastic coast. In: Reading, H.G. (Ed.), Sedimentary Environment: Processes, Facies and Stratigraphy. Blackwell Publ., pp. 154–231
Reinson, G.E., 1992. Transgressive barrier island and estuarine systems. In: Walker, R.G., James, N.P. (Eds.), Facies Models-Response to Sea Level Change. Geological Association of Canada Publications, pp. 179–194.
Rocha-Campos, A.C., Basei, M.A.S., Nutman, A.P., Santos, P.R., Passarelli, C.R., Canile, F. M., Fernandes, M.T., Ana, H.S., Veroslavky, G., 2019. U-Pb zircon dating of ash fall deposits from paleozoic Paraná Basin of Brazil and Uruguay: a reevaluation of the stratigraphic correlations. J. Geol. 127 (2), 167–182.
Schmidt-Neto, H., Netto, R.G., Dasguptab, S., 2018. Storm-related taphofacies in estuarine settings: an integrated analysis on the early permian deposits of the Rio Bonito Formation (Paraná Basin, S Brazil). J. S. Am. Earth Sci. 85, 263–277.
Schnurrenberger, D., Russell, J., Kelts, K., 2003. Classification of lacustrine sediments based on sedimentary components. J. Paleolimnol. 29, 141–154.
Schopf, J.M., 1956. A definition of coal. In: Economic Geology, vol. 51, pp. 521–527, 6.
Schubel, J.R., Hirschberg, D.J., 1978. Estuarine graveyards, climatic change, and the importance of the estuarine environment. In: Estuarine Interactions. Academic Press, pp. 285–303.
Shaw, J., You, Y., Mohrig, D., Kocurek, G., 2015. Tracking hurricane-generated storm surge with washover fan stratigraphy. Geology 43 (2), 127–130.
Silva, M.B., Kalkreuth, W., 2005. Petrological and geochemical characterization of Candiota coal seams, Brazil — implication for coal facies interpretations and coal rank. Int. J. Coal Geol. 64, 217–238.
Smith, J.W., Batts, B.D., 1974. The distribution and isotopic composition of sulfur in coal. Geochem. Cosmochim. Acta 38, 121–133.
Takahashi, T., 2007. Debris Flow: Mechanics. Prediction and Countermeasures, London, p. 154.
Takahashi, T., 2009. A review of Japanese debris flow research. Int. J. Eros. Contr. Eng. 2 (1), 1–14.
Tape, C.H., Cowan, C.A., Runkel, A.C., 2003. Tidal-bundle sequences in the Jordan Sandstone (Upper Cambrian), southeastern Minnesota, U.S.A.: Evidence for tides along inboard shorelines of the Sauk Epicontinental Sea. J. Sediment. Res. 354–366.
Tedesco, J., Cagliari, J., Chemale Jr., F., Lana, C., 2019. Provenance and paleogeography of the Southern Paraná Basin: Geochemistry and U-Pb zircon geochronology of the Carboniferous-Permian transition. Sediment. Geol. 393-394, 105539.
Tessier, B., 2012. Stratigraphy of tide-dominated estuaries. In: Davis, R.A., Dalrymple, R. W. (Eds.), Principles of Tidal Sedimentology. Springer, Dordrecht, pp. 109–128.
Tjallingii, R., Stattegger, K., Wetzel, A., Phach, P.V., 2010. Infilling and flooding of the Mekong River incised valley during deglacial sea-level rise. Quat. Sci. Rev. 29, 1432e1444.
Trentin, F.A., Lavina, E.L.C., Silveira, A.S., Silva, V.E., Lopes, S.R.X., Lopes, A.A.O., Faccion, J.E., 2019. 3D stratigraphic forward modeling of an ancient transgressive barrier system: A case study of accuracy and sensitivity. Mar. Petrol. Geol. 109, 675–686.
Van de Meene, J.W.H., Boersma, J.R., Terwindt, J.H.J., 1996. Sedimentary structures of combined flow deposits from the shoreface-connected ridges along the central Dutch coast. Mar. Geol. 131, 151–175.
Wiberg, P.L., Harris, C.K., 1994. Ripple geometry in wave dominated environments. J. Geophys. Res. 99, 775–789.
Wildner, W., Ramgrab, G.E., Lopes, R.C., Iglesias, C.M.F., 2006. Mapa Geológico Do Estado Do Rio Grande Do Sul. 1:750000. CPRM, Serviço Geológico Do Brasil. Porto Alegre, RS.
Yeste, L.M., Henares, S., McDougall, N., García-García, F., Viseras, C., 2018. Towards the multi-scale characterization of braided fluvial geobodies from outcrop, core, ground-penetrating radar and well log data. Geol. Soc. Londn. Special Public. 488, 73–95.
Zalán, P.V., Wolff, S., Astolfi, M.A.M., Vieira, I.S., Conceição, J.C.J., Appi, V.T., Neto, E. V.S., Cerqueira, J.R., Marques, A., 1990. The Paraná Basin, Brazil. AAPG Memoir 51, 681–708.